*Catalysis Reviews, 47:257–296, 2005*

*ISSN: 0161-4940 print*
*DOI: 10.1081/CR-200057488*

Taylor & Francis
Taylor & Francis Group

# Recent Advances on $TiO_2$-$ZrO_2$ Mixed Oxides as Catalysts and Catalyst Supports

Benjaram M. Reddy and Ataullah Khan

Inorganic and Physical Chemistry Division, Indian Institute of Chemical Technology, Hyderabad, India

This is the first review of titanium dioxide-zirconium dioxide ($TiO_2$-$ZrO_2$) mixed oxides, which are frequently employed as catalysts and catalyst supports. In this review many details pertaining to the synthesis of these mixed oxides by various conventional and nonconventional methods and their characterization by several techniques, as reported in the literature, are assessed. These mixed oxides have been synthesized by different preparative analogies and were extensively characterized by employing various spectroscopic and nonspectroscopic techniques. The $TiO_2$-$ZrO_2$ mixed oxides are also extensively used as supports with metals, nonmetals, and metal oxides for various catalytic applications. These supported catalysts have also been thoroughly investigated by different techniques. The influence of $TiO_2$-$ZrO_2$ on the dispersion and surface structure of the supported active components as examined by various techniques in the literature has been contemplated. A variety of reactions catalyzed by $TiO_2$-$ZrO_2$ and supported titania-zirconia mixed oxides, namely; dehydrogenation, decomposition of chlorofluoro carbons (CFCs), alcohols from epoxides, synthesis of $\varepsilon$-caprolactam, partial oxidation, deep oxidation, hydrogenation, hydroprocessing, organic transformations, $NO_x$ abatement, and photo catalytic VOC oxidations that have been pursued in the literature are presented with relevant references.

**Keywords** $TiO_2$-$ZrO_2$ mixed oxide, $ZrTiO_4$, Coprecipitation, Sol-gel, Acid-base properties, Dehydrogenation, Decomposition of CFCs, Oxidation, Hydrogenation, Hydroprocessing, Organic transformations, $NO_x$ abatement, Photo catalytic activity

Received October 27, 2004; accepted January 28, 2005
Address correspondence to Dr. Benjaram M. Reddy, Inorganic and Physical Chemistry Division, Indian Institute of Chemical Technology, Uppal Road, Hyderabad 500 007, India. E-mail: bmreddy@iict.res.in or mreddyb@yahoo.com

## 1. INTRODUCTION AND SCOPE OF THIS REVIEW

Metal oxides represent one of the most important and widely employed categories of solid catalysts, either as active phases or supports. Metal oxides are utilized both for their acid-base and redox properties and constitute the largest family of catalysts in heterogeneous catalysis (1–4). Among various metal oxide catalysts, the combination of titania-zirconia has attracted much attention in recent years. These mixed oxides have been extensively used as catalysts and catalyst supports for a wide variety of reactions as summarized in Table 1 (5–66). In addition to catalytic applications, these mixed oxides have also been employed for various other purposes such as photoconductive thin films, gas sensors, and in fuel cell and ceramic technologies. Interestingly, both titanium dioxide ($TiO_2$) and zirconium dioxide ($ZrO_2$) single oxides exhibit excellent catalytic properties for various reactions and both have been used as supports to disperse various noble and transition metals for distinct catalytic applications. The $TiO_2$ is unique for its photocatalytic and strong metal support interaction (SMSI) properties (67, 68) and the $ZrO_2$ is a well-known solid acid catalyst (69) and both of them are n-type semiconductors.

It is established in the literature that mixing two dissimilar oxides adds another parameter since they are liable to form new stable compounds, which can lead to totally different physicochemical properties and catalytic behavior. Such advanced titania-zirconia mixed oxides not only take advantage of both $TiO_2$ (active catalyst and support) and $ZrO_2$ (acid-base properties), but also extend their application through the generation of new catalytic sites due to a strong interaction between them. In fact, the facile formation of zirconium titanate ($ZrTiO_4$) compound between $ZrO_2$ and $TiO_2$ exhibits excellent catalytic properties for various reactions as listed in Table 1.

The $TiO_2$-$ZrO_2$ composite oxides exhibit high surface area, profound surface acid-base properties, a high thermal stability, and strong mechanical strength (8–10). It is an established fact in the literature that active components dispersed on mixed metal oxides often produce superior catalysts to the one supported on single oxides for a number of reactions (70). It is known from modern catalytic surface science studies that the nature and quality of a carrier material is a key part of the catalyst. Defined properties and consistent quality of the support material are a prerequisite for a successful catalyst. Although $TiO_2$-$ZrO_2$ binary oxides have been extensively employed for various purposes in different domains, there is no review in the literature on their synthesis, physicochemical properties, and catalytic applications. To the best of our knowledge, this will be the first review covering the existing literature and emphasizing the significance of these mixed oxides and their utility in the area of catalysis.

**Table 1:** Summary of various reactions catalyzed by titania-zirconia mixed oxides as catalysts and catalyst supports.

| Catalysts | Preparation method | Reactions | Refs. |
|---|---|---|---|
| $TiO_2$-$ZrO_2$ | Coprecipitation | Isomerization of 1-methyl cyclohexene oxide | (5) |
| $TiO_2$-$ZrO_2$ | Coprecipitation | Isomerization of cyclohexene oxide | (6) |
| $TiO_2$-$ZrO_2$ | Coprecipitation | Isomerization of 2-carene and allylalcohol | (7) |
| $TiO_2$-$ZrO_2$ | Coprecipitation | Nonoxidative dehydrogenation of ethylbenzene | (8,9) |
| $TiO_2$-$ZrO_2$ | Coprecipitation | Nonoxidative dehydrogenation of ethylcyclohexane | (10) |
| $V_2O_5$-$TiO_2$-$ZrO_2$ | Coprecipitation | Dehydrogenation of cyclohexane | (11) |
| $TiO_2$-$ZrO_2$ | Coprecipitation | Dehydrogenation of ethylbenzene | (12) |
| $TiO_2$-$ZrO_2$ | Coprecipitation | Dehydrocyclization of $C_6$-$C_8$ n-paraffins | (13) |
| $B_2O_3$/$TiO_2$-$ZrO_2$ | Coprecipitation/impregnation | Beckman rearrangement of cyclohexanone | (14,15) |
| $V_2O_5$/$TiO_2$-$ZrO_2$ | Coprecipitation/impregnation | Methanol partial oxidation | (16,17) |
| $V_2O_5$/$TiO_2$-$ZrO_2$ | Sol-gel/Impregnation | Ethanol partial oxidation | (18) |
| $TiO_2$-$ZrO_2$ | Coprecipitation | Dehydration of methanol to dimethylether | (19) |
| $TiO_2$-$ZrO_2$ | Sol-gel | Selective dehydration of isopropanol to propene | (20) |
| $V_2O_5$/$TiO_2$-$ZrO_2$ | Coprecipitation/Impregnation | Isobutraldehyde from ethanol and methanol | (21,22) |
| $V_2O_5$/$TiO_2$-$ZrO_2$ | Coprecipitation/Impregnation | Anisaldehyde from 4-methylanisole | (23) |
| $TiO_2$-$ZrO_2$ | Sol-gel neutral amine route | Epoxidation of cyclo-octene | (24) |
| Pt/$TiO_2$-$ZrO_2$ | Coprecipitation/Incipient wetness | Soot oxidation | (25) |
| Pd/$TiO_2$-$ZrO_2$ | Coprecipitation/Impregnation | Low temperature methane combustion | (26) |
| Pt/$TiO_2$-$ZrO_2$ | Coprecipitation/Impregnation | Naphthalene hydrogenation | (27) |
| Pt/$TiO_2$-$ZrO_2$ | Sol-gel/Impregnation | Furfural hydrogenation | (28) |
| $TiO_2$-$ZrO_2$ | Coprecipitation | Hydrogenation of carboxylic acids to alcohols | (29) |
| $Y_2O_3$-$TiO_2$-$ZrO_2$ | Coprecipitation | Hydrosulfurization of methanol | (30) |
| $MoS_2$/$TiO_2$-$ZrO_2$ | Sol-gel/Solvo-thermal treatment | Hydrodesulfurization of dibenzothiophene | (31) |
| Ni-Mo/$TiO_2$-$ZrO_2$ | Sol-gel/SCF extraction | Hydroprocessing | (32) |
| $MoO_3$/$TiO_2$-$ZrO_2$ | Coprecipitation/Incipient wetness | Hydroprocessing | (33) |
| $MoO_3$/$TiO_2$-$ZrO_2$ | Sol-gel/Impregnation | Hydroprocessing | (34) |
| $TiO_2$-$ZrO_2$ | Coprecipitation | Preparation of p-mentha-1,8-dien-4-ol | (35) |
| $TiO_2$-$ZrO_2$ | Coprecipitation | Synthesis of chlorobenzene | (36) |
| $SO_4^{2-}$/$TiO_2$-$ZrO_2$ | Coprecipitation/Impregnation | Regioselective synthesis of mononitrochlorobenzene | (37) |

(*continued*)

**Table 1:** Continued.

| Catalysts | Preparation method | Reactions | Refs. |
|---|---|---|---|
| $MoO_3/TiO_2$-$ZrO_2$ | Coprecipitation/Impregnation | Synthesis of diacetates | (38,39) |
| $WO_3/TiO_2$-$ZrO_2$ | Coprecipitation/Impregnation | Cumene dealkylation | (40) |
| $NiSO_4/TiO_2$-$ZrO_2$ | Coprecipitation/Impregnation | Cumene dealkylation | (41) |
| Fe,Mn-$SO_4^{2-}/TiO_2$-$ZrO_2$ | Coprecipitation/Impregnation | Benzene isopropylation | (42) |
| $Pt/TiO_2$-$ZrO_2$ | Coprecipitation/Impregnation | Low temperature SCR of $NO_x$ | (43) |
| $Ag/TiO_2$-$ZrO_2$ | Coprecipitation/Impregnation | SCR of NO with propene | (44) |
| $Ag/TiO_2$-$ZrO_2$ | Coprecipitation/Impregnation | SCR of NO with propene, propanol, and acetone | (45) |
| $Pt/TiO_2$-$ZrO_2$ | Sol-gel/Impregnation | NO reduction with $CH_4$ | (46) |
| Ag, In/$TiO_2$-$ZrO_2$ | Sol-gel/Impregnation | SCR of NO with propene | (47) |
| Pd-In/$TiO_2$-$ZrO_2$ | Coprecipitation/Impregnation | SCR of NO in water vapor | (48) |
| $Pt/TiO_2$-$ZrO_2$ | Coprecipitation/Impregnation | SCR of NO in oxygen | (49) |
| $CuO/TiO_2$-$ZrO_2$ | Coprecipitation/Impregnation | CO + NO reaction | (50) |
| $Pt/TiO_2$-$ZrO_2$ | Wet precipitation | Dual-bed lean deNOx process | (51) |
| $Au/SO_4^{2-}/TiO_2$-$ZrO_2$ | Sol-gel | Catalytic hydrolysis of HCFC-22 | (52) |
| $TiO_2$-$ZrO_2$ | Sol-gel | Decomposition of CFC-113 | (53) |
| $WO_x/TiO_2$-$ZrO_2$ | Sol-gel | Decomposition of CFC-113 | (54) |
| $SO_4^{2-}/TiO_2$-$ZrO_2$ | Sol-gel | Catalytic hydrolysis of CFC-12 | (55) |
| $TiO_2/ZrO_2$ thin films | Sol-gel | Photocatalytic oxidation (PCO) of ethylene | (56) |
| $TiO_2/ZrO_2$ thin films | Sol-gel | PCO of acetone vapor | (57) |
| $Ti_{1-x}Zr_xO_2$ | Citric acid | PCO of acetone vapor in air | (58) |
| $TiO_2/Zr_xTi_{1-x}O_2$ | Sol-gel | Photocatalytic decolorization of methyl orange | (59) |
| $ZrTiO_4$ | Sol-gel | PCO of isopropanol | (60) |
| $ZrTiO_4$ | Sol-gel | PCO of 1,4 pentanediol | (61) |
| $ZrO_2$-$TiO_2$ | Sol-gel | Photocatalytic decomposition-salicylic acid,Cr(VI) | (62) |
| $ZrTiO_4$ | Sol-gel | PCO by laser flash photolysis | (63) |
| $TiO_2/ZrO_2$ | Polymer gel templating | Photo decomposition of salicylic acid, 2ClPhOH | (64) |
| $TiO_2/ZrO_2$ thin films | Sol-gel processing | Catalytic and photo oxidation of ethylene | (65) |
| $ZrTiO_4$ thin films | Dip-coating method | Hydrocarbon gas sensors | (66) |

## 2. PREPARATION OF $TiO_2$-$ZrO_2$ MIXED OXIDES

There are two types of combinations between $TiO_2$ and $ZrO_2$: physically mixed (with interaction forces being nothing more than weak Van der Waals forces) and chemically bonded (i.e., the formation of Ti–O–Zr linkages). When strong interaction results in chemical bonding, the physicochemical and reactivity properties of titania-zirconia mixed oxides will be very different from those of simple combinations of individual oxides (mechanical mixtures). The degree of interaction, or in other words, homogeneity or dispersion, largely depends on the preparation method and the synthesis conditions. Many different preparation methodologies have been employed to synthesize these composite oxides.

The most widely employed methods to prepare $TiO_2$-$ZrO_2$ mixed oxides are coprecipitation (5–17, 19, 21–23, 25–27, 29, 30, 33, 35–45, 48–50) and sol-gel (18, 20, 28, 31, 32, 34, 46, 47, 52–57, 59–63, 71). Other less frequently applied procedures include super critical fluid (SCF) extraction (32), non-hydrolytic modified sol-gel (72), citric acid complex (58), neutral amine (24, 73), and microwave assisted combustion synthesis (74). The supported oxides of $TiO_2$ deposited on $ZrO_2$ substrate, denoted as $TiO_2/ZrO_2$ supported oxides, have also been investigated and were prepared by impregnation, chemical vapor deposition (CVD), atomic layer deposition (ALD), and deposition precipitation methods (75).

An adequate synthetic methodology is a fundamental starting point for developing any viable catalytic material. Among various preparative procedures available as mentioned earlier, coprecipitation has been most widely used, which is also termed wet precipitation in some reports. This particular preparative analogy is well documented in the literature. The precursors (mostly chlorides, oxychlorides, and nitrates) are usually dissolved in aqueous or in anhydrous medium and titrated with a precipitating reagent (urea or aqueous $NH_3$) to obtain the hydroxide gels, which on subsequent calcination yield mixed oxides. Sol-gel hydrolysis is also widely employed due to its capability in controlling the textural and surface properties of the resulting oxides. In sol-gel processes, domain formation due to the difference in the hydrolysis and condensation rates of Ti- and Zr-alkoxides has been identified as a major problem in the preparation of atomically dispersed mixed oxides. The preparation of zirconium titanate powder by a sol-gel route was reported by Navio et al. (71) in which a hydroxoperoxo compound of Zr and Ti (HXPZT) was observed to be the reactive precursor, and this particular preparative strategy also received wide acceptability. Weissman et al. (32) adopted a SCF extraction analogy to obtain $TiO_2$-$ZrO_2$ mixed oxide aerogels. In the SCF method solvents were extracted from the gel without collapsing its structure, as would occur in conventional drying. The result was an aerogel having a high specific surface area. The use of SCF to prepare aerogels for catalytic applications has been elaborated in a recent review (76). Super critical drying

eliminates the liquid-vapor interface, which would exist during conventional drying, thus preventing capillary forces from collapsing the porous material. Through a modified sol-gel process, the so-called neutral amine route, spherical particles of hexagonal 1 : 1 zirconia-titania mixed oxides (1 : 1 mole ratio) were synthesized by De Farias et al. (24, 73). The zirconium(IV) and titanium(IV) butoxides along with 1,12-diaminododecane were employed as precursors in this method. The SEM image of the elegantly synthesized spherical particles of zirconia-titania lamellar oxide by this method is shown in Figure 1. A great advantage of this method is that the reaction takes place in an open system without any special experimental conditions. A sequence of reactions starting with hydrolysis of mixture of alkoxides and ending with the condensation step, to furnish a network structure consisting of both the oxides, was proposed as shown in the form of Eqs. (1) and (2) (73):

$$\mathrm{Ti(OR)_4 \cdot Zr(OR)_4 + 8\ H_2O = Ti(OH)_4 \cdot Zr(OH)_4 + 8\ ROH} \quad (1)$$

$$n\mathrm{Ti(OH)_4 \cdot Zr(OH)_4} + n\mathrm{Ti(OH)_4 \cdot Zr(OH)_4} = (\mathrm{Ti{-}O{-}Zr{-}O{-}Ti{-}O{-}Zr})_n + n\mathrm{H_2O} \quad (2)$$

In sol-gel processes, which are based on cohydrolysis of molecular precursors such as metal alkoxides, the main problem lies in the control of reaction

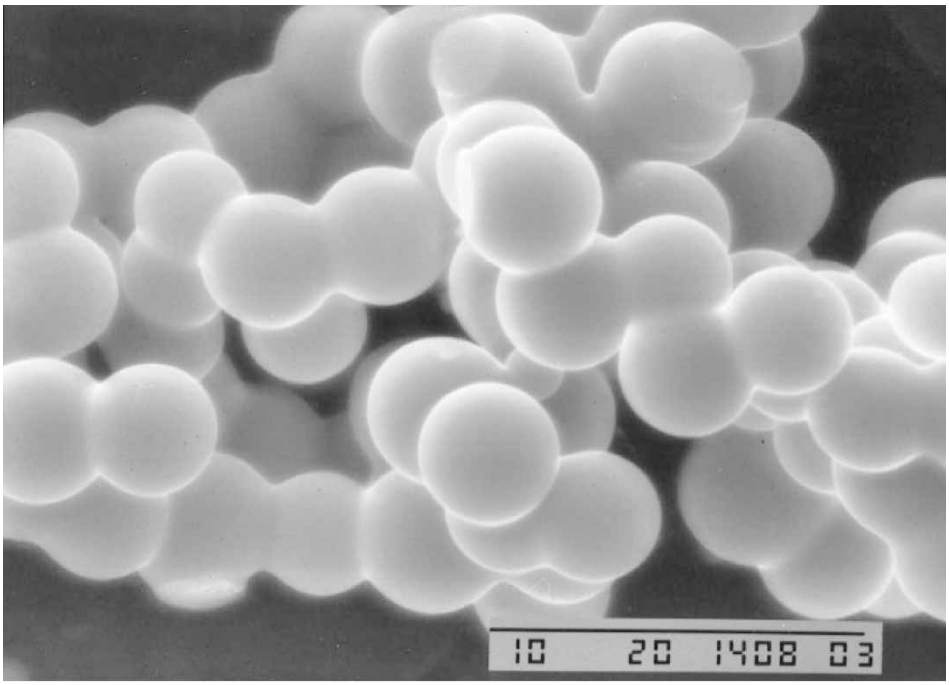


**Figure 1:** The SEM image of 1:1 titania-zirconia spheres calcined at 773 K for 2 h. (From Ref. 73.)

rates, which are highly dependent on the nature of metals. To achieve homogeneous oxides with predetermined compositions, the difference in the reactivity has to be minimized by controlled prehydrolysis of the less reactive precursors or by chemical modification of the precursors. In this context, a chemical route that does not involve hydrolysis was developed. This process is based on the thermal condensation reaction between metal chlorides and metal alkoxides or, alternatively, on the etherolysis of metal chlorides (alkoxide functions being formed in-situ). When metal chlorides and metal alkoxides are mixed, fast-ligand exchange reaction occurs giving rise to a mixture of metal chloroalkoxides (Eq. 3) so that homo- as well as heterocondensation could occur. The zirconium titanate gels were thus synthesized below 973 K without the formation of intermediate $TiO_2$ and $ZrO_2$ phases by a nonhydrolytic sol-gel route (72).

$$MCl_n + M^1(OR)_n \longleftrightarrow MCl_{n-x}(OR)_x + M^1Cl_x(OR)_{n-x} \quad (3)$$

Bartlett et al. (77, 78) reported the preparation of $TiO_2/ZrO_2$ colloids by (i) hydrolysis of a mixture of titanium and zirconium alkoxides and peptization of the resulting hydrolyzate with nitric acid (homogeneous), and (ii) hydrolysis of a titanium alkoxide and peptization of the resulting hydrolyzate with aqueous zirconium (IV) nitrate solution (heterogeneous). It was found that, in the homogeneous colloids, the zirconia is segregated within the matrix of the titania crystallites (on $\sim$1 nm scale), whereas, in the heterogeneous colloids, the zirconia is segregated on the surface of the titania crystallites (on $\sim$10 nm scale) (77). Anderson and coworkers employed yet another approach called the sol-gel processing approach in which the titania and zirconia sols were prepared separately prior to combining (57). The individual sols were stirred continuously for 3 days until peptization was complete, after which the two sols were combined and dialyzed further to obtain $TiO_2/ZrO_2$ thin films. The citric acid complexing route was employed by Yu et al. (58) wherein the precursor ($TiCl_4 + ZrCl_4 +$ citric acid + HCl) mixture was sonicated to produce the $Ti_{1-x}Zr_xO_2$ solid solution.

The ALD techniques are closely related to the CVD method. In ALD, a binary CVD reaction is divided into two separate self-limiting half-reactions. The ALD is achieved by repeating these two self-limiting reactions in an ABAB... sequence. The ALD method was utilized to obtain the atomic layer controlled growth of conformal $TiO_2/ZrO_2$ thin films (75). As shown in Fig. 2, the transmission electron microscopy (TEM) image of the $ZrO_2$ particles coated by $TiO_2$ ALD reveal ultra thin and conformal $TiO_2$ coatings on the $ZrO_2$ particles. The ultra thin $TiO_2$ coatings will be useful in altering the surface of the $ZrO_2$ particles, while allowing the particles to maintain their bulk $ZrO_2$ properties (75). A high-energy mechanical milling procedure was also employed to prepare a $TiO_2$-$ZrO_2$ (1 : 10 mol%) mixed oxide (79). As far

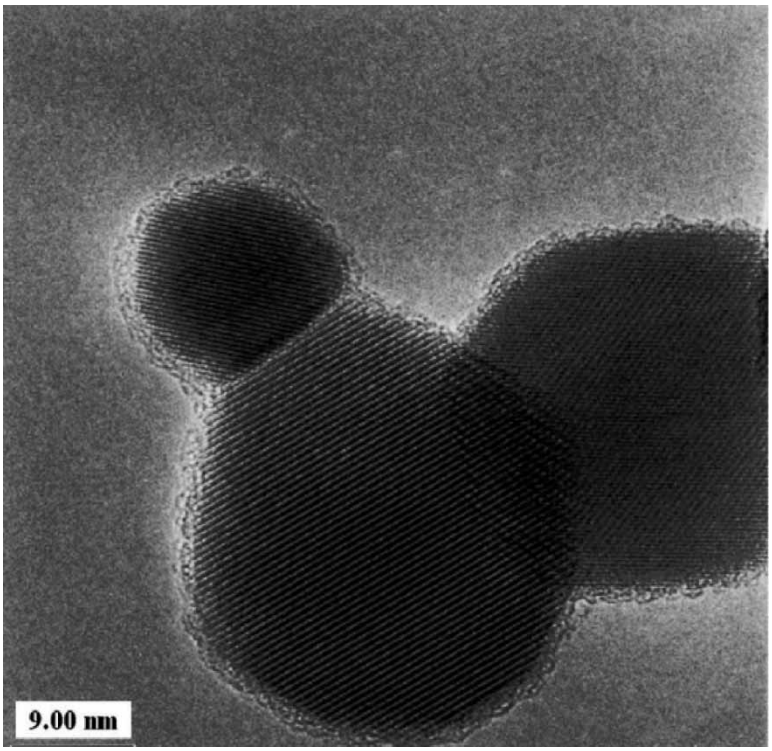


**Figure 2:** The TEM image of $ZrO_2$ particles coated by $TiO_2$ ALD after 40 AB cycles at 600 K. The $ZrO_2$ particles are crystalline and the $TiO_2$ ALD coating is fairly amorphous. (From Ref. 75.)

as the solid-state synthesis and high-energy milling are concerned, these type of synthesis procedures normally lead to the preparation of ceramics, which, by the way is a field where stabilized zirconia are largely employed (79). Ceramic materials feature a high degree of densification and, therefore, sintering, which is exactly the opposite of what the desirable property is for catalytic applications. Hence, materials obtained by these synthetic routes are not recommended for catalytic applications.

Very recently a $ZrTiO_4$ compound was prepared directly by adopting a microwave-assisted combustion synthesis route, wherein the principles of propellant chemistry were utilized (80), with the requisite quantities of in situ generated titanyl nitrate and zirconyl nitrate as the precursors (74). Mesoporous large-pore $ZrTiO_4$ with semicrystalline framework was synthesized using amphiphilic poly(alkylene oxide) block copolymers as structure-directing agents in nonaqueous solutions by Yang et al. (81). A family of various binary oxide compositions including titania-zirconia with a hierarchically bimodal mesoporous-macroporous structure, which exhibit high surface areas and large pore volumes, were reported by Yuan et al. (82) recently. A polymer gel templating technique was employed to make porous metal oxide networks of

$TiO_2/ZrO_2$ (64). The photocatalytic efficiency of these oxides for photodecomposition of salicylic acid and 2-chlorophenol was found to be high (64). The wide-pore $ZrO_2$-$TiO_2$ mixed oxides were also synthesized by a low temperature sol-gel method followed by solvo-thermal treatment, and these materials were found to be highly promising for hydrotreating applications (31).

Due to lack of generally recognized criterion for the detection of homogeneity of mixed oxides, a comparison of different synthesis routes is not easy. In fact the low calcination temperatures often employed to obtain a high surface area sample, do not allow unambiguous detection of a single-phase product. Generally speaking, the sol-gel synthesis by controlled hydrolysis of alkoxides or similar precursors are considered to be a suitable method leading to a high degree of homogeneity. The underlying idea is that the preparation of gel or gel-like precursor should lead to a homogeneous dispersion at molecular level of Ti and Zr species, which upon calcination will lead to intimately formed mixed oxides.

## 3. STRUCTURAL CHARACTERISTICS

### 3.1 $TiO_2$-$ZrO_2$ Mixed Oxides

A wide range of techniques [X-ray diffraction (XRD), diffuse reflectance infared Fourier transform spectroscopy (DRIFTS), differential thermal analysis/thermo gravimetric analysis (DTA/TGA), temperature programmed desorption/reduction (TPD/TPR), Fourier transform infared (FTIR), Raman spectroscopy (RS), electron spin resonance (ESR), solid-state nuclear magnetic resonance (NMR), X-ray photoelectron spectroscopy (XPS), scanning electron microscopy (SEM), transmission electron microscopy (TEM), etc.] were described in the literature to characterize $TiO_2$-$ZrO_2$ and metal or metal--oxide impregnated $TiO_2$-$ZrO_2$ mixed oxides (8–10, 16, 17, 24, 32, 34, 44, 70–75, 83–96). As described earlier, the titania-zirconia mixed oxides are most commonly obtained by calcining the $Ti(OH)_4$-$Zr(OH)_4$ hydroxide gels derived through the precipitation of the corresponding precursor salt solutions. As shown in Fig. 3, the X-ray powder diffraction pattern of a low-temperature calcined sample reveal that it is in an X-ray amorphous state. Upon high temperature treatment, prominent diffraction lines due to the zirconium titanate ($ZrTiO_4$) phase are mainly manifested (8–10, 13). Wang and coworkers (8–10), from the X-ray diffraction study of $TiO_2$-$ZrO_2$ samples having different compositions and calcined at 623 K, reported that the $TiO_2$-$ZrO_2$ mixed oxide becomes amorphous if neither the content of $TiO_2$ nor $ZrO_2$ are less than 25%. The $TiO_2$-$ZrO_2$ was amorphous when it was calcined at a temperature below 623 K and the crystalline $ZrTiO_4$ was noted beyond 723 K. The crystallinity of the $ZrTiO_4$ increased with increasing calcination temperature up to 1173 K. However, some $TiO_2$-rutile phase was separated out from $ZrTiO_4$ when the

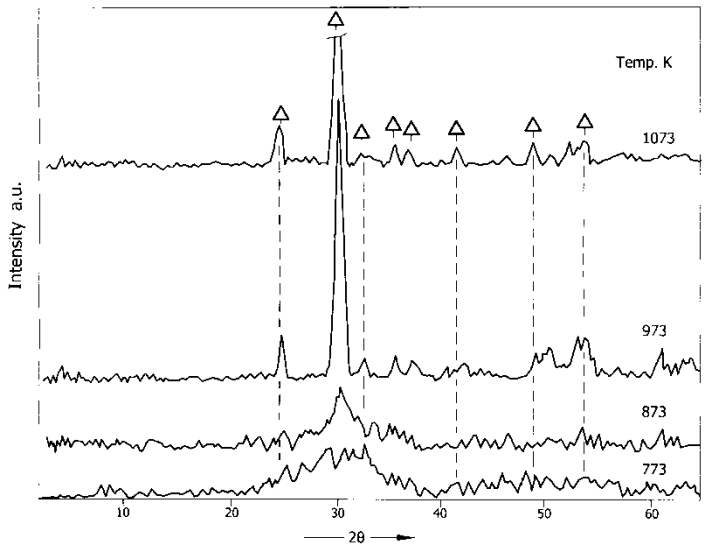


**Figure 3:** X-ray powder diffraction patterns of $TiO_2$-$ZrO_2$ calcined at various temperatures: (△) lines due to $ZrTiO_4$. (From Ref. 70.)

calcination temperature exceeded 1123 K. Noguchi and Mizuno (97) reported that monoclinic and tetragonal $ZrO_2$ could be formed by the decomposition of $ZrTiO_4$ when it was quenched from 2673 K to 2373 K. Navio et al. (71), who employed a modified sol-gel procedure, reported the formation of $ZrTiO_4$ phase at 923 K. Tajima et al. (53) also investigated the XRD patterns of various $TiO_2$-$ZrO_2$ binary oxides having different compositions. An amorphous phase was observed for TZ-55/45 composition and the crystalline $ZrTiO_4$ for TZ-58/42. The TZ-70/30, TZ-82/18, and TZ-90/10 compositions were mixtures of $ZrTiO_4$ and the anatase-type $TiO_2$ crystals (53).

The $ZrTiO_4$ compound formation was discovered long back while studying phase equilibria in the $ZrO_2$ and $TiO_2$ systems (98–101). The $ZrTiO_4$ was obtained by solid state reaction between equimolar mixtures of these oxides at high temperatures. It is a stable compound in the phase diagram of $TiO_2$ and $ZrO_2$. The $ZrTiO_4$ compound belongs to the space group *Pbcn* and has an orthorhombic structure ($\alpha$-$PbO_2$) with complete disorder of the $Zr^{4+}$ and $Ti^{4+}$ ions on the metal sites (101, 102). The crystal structure consists of an edge shared metal-oxygen octahedra [$MO_6$], which is quite distorted. The $ZrTiO_4$ also fulfils the necessary conditions for determination of the homogeneity of the gel precursors from its crystallization behavior. When a high homogeneity level is not achieved, crystallization of the $TiO_2$ is observed before the crystallization into the $ZrTiO_4$ below 973 K (8–10).

In comparison to single oxides ($TiO_2$, S.A = 20–200 $m^2 g^{-1}$; $ZrO_2$, S.A = 30–160 $m^2 g^{-1}$), the composite oxides ($TiO_2$-$ZrO_2$, S.A = 85–430 $m^2 g^{-1}$)

exhibit high surface area, strong surface acidity, and high thermal and mechanical strength. Since titanium and zirconium belong to the same group (IVB), they are expected to have similar physicochemical properties. When their oxides are precipitated together, the mutual interaction between them is expected to be profound, which inhibits their individual crystallization. The observed significant changes in the specific surface area, acidity, basicity, and catalytic activity could be due to this strong mutual interaction. With the addition of zirconia to titania, the surface area of the mixed oxide increases sharply and reaches a maximum value for the mixed oxide having a Ti and Zr molar ratio of 1 : 1. The addition is also known to influence the crystallization pattern of both the oxides. In fact, they crystallize at higher temperatures when compared to that of single oxides (8–10, 16, 17, 88, 89).

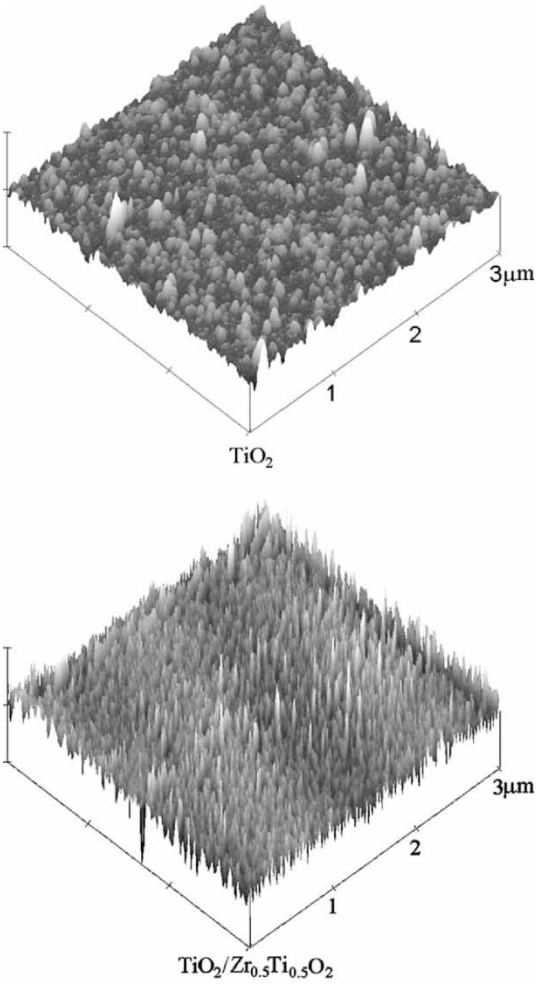


**Figure 4:** The AFM images of pure and composite $TiO_2$ films. (From Ref. 59.)

The surface morphology and average surface roughness of $TiO_2/ZrO_2$ films were characterized by atomic force microscopy (AFM) (59). The AFM images presented in Fig. 4 revealed that the surface morphology of the composite film is very different from that of pure $TiO_2$ film. The crystallite size of the composite film is much smaller than that of pure $TiO_2$ film, which indicates that the introduction of intermediate layers suppresses the crystallite growth of $TiO_2$. As a result, nanometer films with smaller crystallite size are easily obtained. In addition, the average surface roughness of pure $TiO_2$ film is 1.487 nm, while that of composite film is 3.313 nm. The greater roughness is due to the discrepancy of the crystal lattices between $Zr_xTi_{1-x}O_2$ and $TiO_2$ (59).

## 3.2 Acid-Base Properties

The acid-base properties of oxide catalysts are very important for the development of scientific criteria in catalytic applications. The conversion and selectivity of a reaction not only depends on the nature of active sites, but also on their strength and number. Tanabe and co-workers investigated the acid-base properties of several binary metal oxides (103–106). Their study sought to develop a theoretical basis for the generation of acidity in various binary oxides, which is nonexistent in the constituent single oxides. A fairly good correlation was demonstrated between the observed highest acid strengths and the average electronegativities of metal ions of the binary oxides (103–106). In the literature various models also have been attempted to predict the formation of new acid sites in various mixed oxides. However, in view of their wider acceptability, Tanabe's and Kung's models have received much more attention in the literature (1, 103–107).

Tanabe's model applies to dilute mixed oxides where a small amount of a second oxide is incorporated into the first oxide by cation substitution. This model assumes that the generation of new acid sites is caused by an excess of negative or positive charge in a model structure of the binary oxide. The model structure constructed is as follows: (i) the coordination number of a cation of the component oxide is maintained in the binary oxide, and (ii) the coordination number of the oxygen ion in the binary oxide is the same as in the major component oxide. This model has been applied to many binary oxides including $TiO_2$-$ZrO_2$. The $TiO_2$-$ZrO_2$ binary oxide has shown affirmative results. The high success rate makes this model highly useful, although it is limited by the assumptions used. One limitation is the need to have a unique coordination number, which may be difficult to decide in systems of low symmetry. Another limitation is the use of formal oxidation states, which may be quite different from the real charge. Since electron deficiency at a site refers to real charge at the site, the use of formal oxidation states may not be accurate. Finally, the model cannot predict acid strength. However,

there appears to be a rough correlation between electronegativity of the cations and the strength of acid sites in many mixed oxides (103, 106).

Another model proposed by Kung takes a rather different approach (1, 107). In Tanabe's model, charge compensation at the substituting ion site by neighboring oxygen ions is important. In Kung's model, a change in electrostatic potential experienced by the substituting cation due to all the ions in the matrix oxide is important. Thus, Tanabe's model is a localized one, and Kung's model is a delocalized one. In Kung's model (1, 107), the difference $\Delta V$ between the electrostatic potentials experienced by a cation A in a matrix $BO_z$ and in $AO_y$ is given by:

$$\Delta V = \Sigma_i(q_i/r_i)_{BO} - \Sigma_i(q_i/r_i)_{AO} \tag{4}$$

where $q_i$ is the charge of the ion at a distance, $r_i$, from the cation A. The subscripts BO and AO denote the matrices $BO_z$ and $AO_y$, respectively. When $\Delta V$ is negative, cation A in the matrix $BO_z$ experiences a more negative potential than in $AO_y$. It will be electrostatically more stable. Therefore, the electron energy levels of cation A are lower in energy in the matrix $BO_z$ and the cation can accept electrons more readily. It will act as a new Lewis acid site. When $\Delta V$ is positive, A is less readily accepting electrons in matrix $BO_z$ than it is in matrix $AO_y$. No new Lewis acid site is generated at the substituting A cation.

The interaction between the two oxides results in a significantly greater surface acidity than that of the single component oxides. As shown in Fig. 5, the single oxides $TiO_2$ and $ZrO_2$ exhibit less surface acidity, as measured by

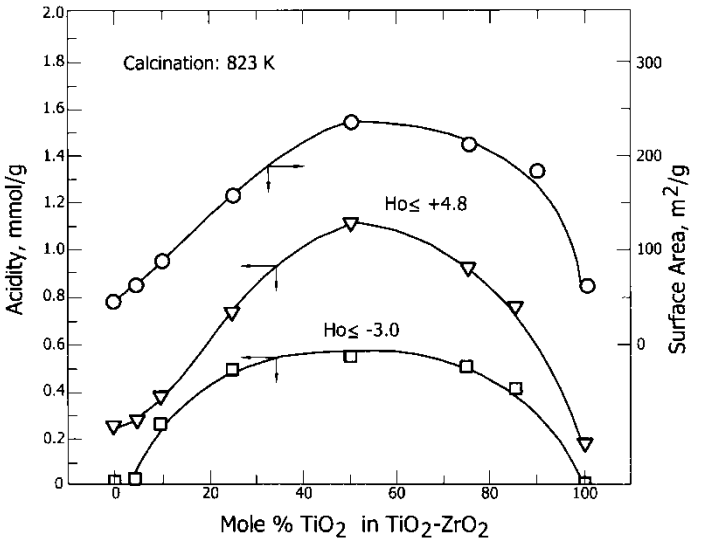


**Figure 5:** Surface area and acidity of $TiO_2$-$ZrO_2$ at various compositions; (○), surface area; (▽), acid strength $H_0 \leq +4.8$; (□), acid strength $H_0 \leq -3.0$. (From Ref. 8.)

Hammett indicators, while the mixed oxides possess various degrees of increased surface acidity, with the maximum occurring at about 50 wt.% $TiO_2$ ($TiO_2/ZrO_2 = 1/1$) (8). These findings are consistent with the model of Tanabe (104) where new acid sites are associated with Ti–O–Zr linkages. It is also quite possible that as the transition metal oxide particle size decreases, the number of surface oxygen anion vacancies increases, hence new and stronger acid sites are created, with the particles of smallest diameter having the strongest acidity (8). The $TiO_2$-$ZrO_2$ mixed oxides can be thought of as a mixture of relatively small particles contributing acidity from anion vacancies, in addition to the surface acidity arising from interactions postulated by Tanabe.

The acid-base characteristics of $TiO_2$-$ZrO_2$ and the corresponding variously promoted samples were extensively investigated using different test reactions (8–10, 103, 108), such as TPD (14, 109), in-situ FTIR (44, 45, 47), and other techniques (41, 45). Nearly two decades ago, Tanabe and co-workers (103) investigated the acidic properties of several binary oxides by n-butylamine titration with various acid-base indicators. A fairly good correlation was demonstrated between the observed highest acid strengths and the average electronegativities of metal ions in the binary oxides. The surface acid-base properties of $TiO_2$-$ZrO_2$ were measured by a calorimetric titration method using n-butylamine and trichloroacetic acid as titrating base and acid, respectively (110). The acid amount and acid strength of $TiO_2$-$ZrO_2$ (1 : 1 molar ratio) were observed to be the largest and highest. Microcalorimetry is another excellent technique employed to obtain information on the acid-base properties of various catalysts by measuring differential molar enthalpy of adsorption using different adsorbents such as ammonia, pyridine, n-butylamine, $CO_2$, and $SO_2$ (111). The surface acidic properties of $B_2O_3/TiO_2$, $B_2O_3/ZrO_2$, and $B_2O_3/TiO_2$-$ZrO_2$ catalysts were examined by $NH_3$-TPD (14). The temperature programmed desorption profiles revealed that the acid strength of the catalysts increases with an increase in zirconia content in the mixed oxide, as was indicated by a continuous shift of the desorption peak of the maximum height to higher desorption temperatures. The $TiO_2$-$ZrO_2$ mixed oxide has much higher acidity and basicity than do the parent oxides, $TiO_2$ and $ZrO_2$ (14, 109). As can be noted from Table 2, the number of acid sites as determined

**Table 2:** Ammonia adsorption on $TiO_2$, $ZrO_2$ and $TiO_2$-$ZrO_2$ mixed oxides (20).

| Catalysts | μmole $NH_3$/g |
|---|---|
| $TiO_2$ | 173 |
| $TiO_2$-$ZrO_2$ (90–10) | 1326 |
| $TiO_2$-$ZrO_2$ (50–50) | 1456 |
| $TiO_2$-$ZrO_2$ (10–90) | 1226 |
| $ZrO_2$ | 138 |

by $NH_3$-TPD increased dramatically in the case of $TiO_2$-$ZrO_2$ mixed oxides (20). To demonstrate the catalytic function of acidic and basic sites on $TiO_2$-$ZrO_2$, $K_2O$ and $H_3BO_3$ were introduced by the wet impregnation method by Fung and Wang (108). It was concluded from their systematic studies that both $K_2O$ and $B_2O_3$ poisons the active sites of the $TiO_2$-$ZrO_2$ catalysts. The thermogravimetric analysis (TGA) studies suggested that doping with $K_2O$ decreases the acid amount while $B_2O_3$ decreases the base amount at the solid surfaces. Fung and Wang further proposed that the number of acid and base sites on $TiO_2$-$ZrO_2$ could be adjusted by doping with small amounts of $K_2O$ and $B_2O_3$ (109). Quantification of the changes in acid-base amounts and their respective strengths were investigated by ammonia and acetic acid TPD measurements (109). Doping with 0.5–2.0 wt.% $B_2O_3$ did not change the base strength, but it decreased the base amount. Doping with 0.5–2.0 wt.% $K_2O$ lead to a decrease of both acid amount and its strength (109).

## 3.3 Metals Supported on $TiO_2$-$ZrO_2$

Various metals (Pt, Ag, In, etc) deposited over $TiO_2$-$ZrO_2$ were employed for different catalytic applications such as hydrogenation, soot oxidation, and de$NO_x$ process (Table 1). Supported metals generally exhibit strong tendency for chemisorption of $H_2$, $O_2$, CO, and light hydrocarbons. Therefore, these catalysts are often employed for hydrogenation-dehydrogenation reactions and several other reactions involving hydrocarbons or CO. It is an established fact in the literature that the dispersion of a metal over a support is generally determined by the amount of $H_2$ or CO chemisorbed (112). The degree/extent of metal dispersion is defined as the ratio of surface metal atoms to the total metal atoms in the catalyst. The higher the dispersion, the higher the efficiency. The uptake of hydrogen could be significantly affected by altering the prereduction temperature. At higher reduction temperatures the dispersed metal particles agglomerate, thus suppressing the uptake of hydrogen. Although restoring the uptake of hydrogen through the irreversible sintering process is difficult, different behaviors are observed for reducible ($TiO_2$) and nonreducible oxides ($Al_2O_3$ and $SiO_2$) (112–114). The uptake of hydrogen on Pt/$TiO_2$ could be restored by reoxidation followed by low-temperature reduction. This phenomenon, including geometric and electronic effects, has been extensively investigated. Nevertheless, most of the time no clear distinction between the electronic effects and the geometric effects is accomplished and they are together labeled as strong metal support interaction (SMSI) (67, 68). The SMSI effect suppresses the hydrogen chemisorption capacity and reduces the catalytic activity of the metal in reactions such as the hydrogenation of hydrocarbons. Lu et al. (28) investigated the electronic effect of Pt on $TiO_2$-$ZrO_2$ binary oxide with various Ti/Zr ratios, without disturbing geometric effect. Significant interaction between the dispersed Pt metal and

the $TiO_2$-$ZrO_2$ support was observed. Addition of $ZrO_2$ to $TiO_2$ prevents the migration of $TiO_2$ onto the metal surface, thereby maximally reducing the geometric effect. For Pt/$TiO_2$-$ZrO_2$ (1 : 1), the relative hydrogen uptake did not fall significantly after high temperature reduction since $ZrO_2$ is very stable and prevents the migration of $TiO_x$ fragments. In this situation it was assumed that there is no loss in the number of metallic active sites ($A_M$) as well as metal-oxide interfacial sites ($A_S$). However, the drop in the relative reaction rate was obviously greater than the fall in the relative hydrogen uptake, implying that the electronic interaction between the support and the metal is strong, which pulls the electrons from metal to the oxide. It would retard the rate of spillover of hydrogen atoms. The diffusion of hydrogen atoms from the platinum particles to the surrounding support surface during the formation of protons and reduced titanium ions is related to the so-called spillover phenomenon. Some studies have concluded that the concentration of oxygen atoms (or hydroxyl groups) on the support surface affect the rate of hydrogen spillover. The higher concentration of oxygen atoms implies a higher rate of hydrogen spillover. The change in the surface structure of $TiO_2$-$ZrO_2$ during reduction treatment by $H_2$, proposed by Wu and coworkers (8, 9) is as follows:

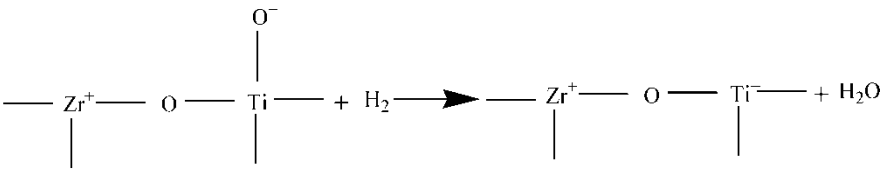


According to them, some oxygen atoms are removed by deep reduction. However, acidity and basicity of $TiO_2$-$ZrO_2$ (1 : 1) did not change significantly after reduction. Therefore, the adsorptivity of the aromatic reactant should not decrease and, thereby, lead to a decline in reactivity. Consequently, the loss of reactivity of high-temperature reduced Pt/$TiO_2$-$ZrO_2$ (1 : 1) was reasonably explained by the slowdown of hydrogen spillover, originating from the removal of oxygen atoms on the surface of the oxide support. The concentration of oxygen atoms decreases as the concentration of $ZrO_2$ increases because the structure of $TiO_2$-$ZrO_2$ is such that each oxygen atom is accompanied by a Ti atom.

The Pt/$TiO_2$-$ZrO_2$ combination catalysts were also reported to be effective in promoting the low temperature $NO_x$-$H_2$ reaction in the presence of excess $O_2$ (43). The high NO-$H_2$ selectivity was primarily a result of oxidative adsorption of NO as nitrate, which completely covers the Pt surface to interfere with $H_2$-$O_2$ combustion at lower temperatures. The NO conversion to $N_2$/$N_2O$ was also found to be very sensitive to the pretreatment, i.e., a reduced catalyst exhibited much higher activity than did an oxidized catalyst. The effect of pretreatment is consistent with the reactivity of nitrate formed on the Pt surface toward $H_2$.

When silver was incorporated into the $TiO_2$-$ZrO_2$, the NO reduction activity by propene enhanced drastically (44, 45). The silver additive effect was explained by the assumption that silver promotes the reaction of $NO_2$ with propene, which is the initial rate-determining step, to form a partially oxidized hydrocarbon. The presence of water vapor suppressed the catalytic activity of $Ag/TiO_2$-$ZrO_2$ for NO reduction by propane due to the formation of oxygenated intermediates (45). On the other hand, when propene was replaced by other oxygenated compounds like 2-propanol and acetone, the $Ag/TiO_2$-$ZrO_2$ showed an excellent catalytic performance for NO reduction (45). In contrast, the presence of water vapor promoted NO reduction activity. It was presumed that water vapor accelerates the selective reduction of NO by suppressing the undesirable oxidation of the reductants by $O_2$. The reaction mechanism of NO reduction by propene in the presence of oxygen over $Ag/TiO_2$-$ZrO_2$ was studied by means of in-situ Fourier transform infrared, combined with catalytic activity studies (44). According to the mechanism, the organic nitro- and nitrite compounds formed initially on the $TiO_2$-$ZrO_2$ support are converted on Ag sites to isocyanate, which is then reduced to $N_2$ by reaction with $NO_2$. In a systematic study, Haneda and coworkers investigated a 5 wt.% $Ag/TiO_2$-$ZrO_2$ sample by TEM technique to estimate the particle size of silver (45). They found that silver is well dispersed on the $TiO_2$-$ZrO_2$ surface with a particle size range of ca. 50–100 nm.

## 3.4 Metal Oxides Supported on $TiO_2$-$ZrO_2$

The influence of dispersed vanadium oxide on thermal stability, physicochemical, and catalytic properties of titania-zirconia binary oxides was extensively investigated using different techniques by Reddy et al. (16, 17, 70, 85–89) and others (18). Vanadium oxide is known to accelerate the phase transformation of $TiO_2$-anatase (A) into rutile (R) in $V_2O_5/TiO_2$ catalysts and also results in the formation of $V_xTi_{1-x}O_2$ solid solutions at 623 K and above treatment temperatures (115, 116). However, in the case of $TiO_2$-based mixed oxides ($TiO_2$-$SiO_2$ and $TiO_2$-$ZrO_2$) the crystallization and phase transformation of anatase to rutile ceased to a certain extent due to the formation of Td and Oh Ti-sites (117, 118). Also a selective formation of $ZrV_2O_7$ compound was observed in the case of $V_2O_5/TiO_2$-$ZrO_2$ samples when calcined at higher temperatures due to a strong interaction between the dispersed vanadium oxide and the $ZrO_2$ portion of the mixed oxide. The $ZrV_2O_7$ formation was accompanied by a $TiO_2$-rutile phase that is released from the binary oxide (88, 89). In particular, the solid state $^{51}V$ and $^{1}H$ MAS NMR studies provided strong evidence about the formation of dispersed and crystalline vanadium oxide phases over the $TiO_2$-$ZrO_2$ support as a function of $V_2O_5$ loading (1–16 wt.%) and also the interaction of the dispersed vanadium oxide with support though the support surface hydroxyl groups (16, 89). The solid

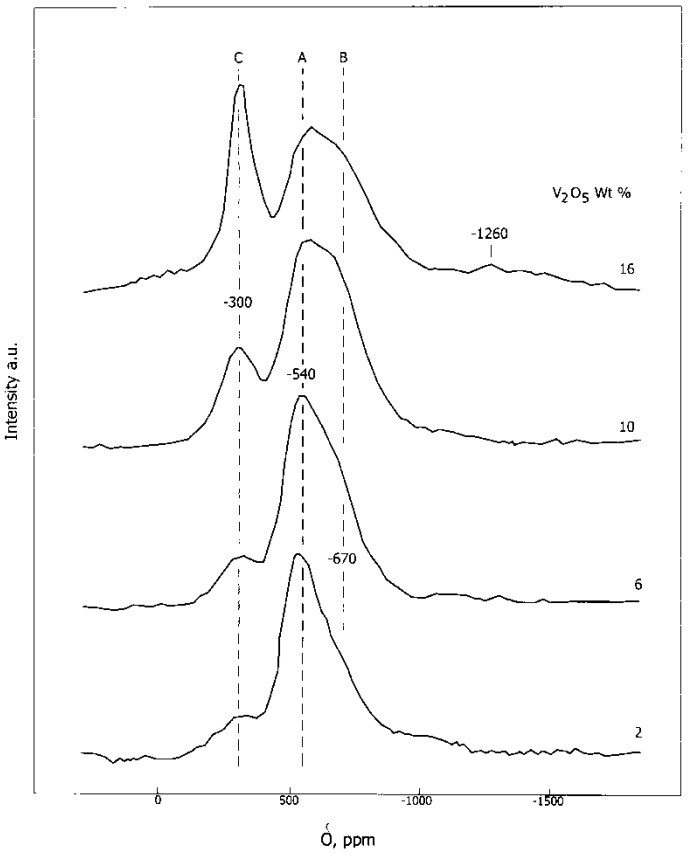


**Figure 6:** Solid-state $^{51}V$ NMR spectra of $V_2O_5/TiO_2$-$ZrO_2$ catalysts. Spectra were obtained without evacuation of the samples. Reproduced from Ref. 89 with permission from ACS.

state $^{51}V$ NMR spectra of the samples as presented in Figs. 6 and 7 revealed the existence of two types of dispersed surface vanadium oxide complexes in a tetrahedral oxygen environment at lower vanadium loadings and a three-dimensional crystalline $V_2O_5$ in a distorted octahedral environment at higher vanadium contents and their distribution was highly sensitive to the evacuation treatment (adsorbed water). The proton $^1H$ MAS NMR results provided evidence for the existence of metal-oxide support-oxide interaction through the support surface hydroxyl groups (89). Park et al. (90) also reported the solid state $^{51}V$ NMR spectra of the vanadium oxide supported on $TiO_2$-$ZrO_2$. Their investigations revealed that the impregnated vanadium oxide was in a highly dispersed state for the samples containing below 25 wt.% $V_2O_5$. However, for the samples containing more than 25 wt.%, the vanadium oxide was in a well-crystallized form due to an excess loading of more than monolayer coverage of the $TiO_2$-$ZrO_2$ support. The formation $ZrV_2O_7$ compound was noted at 773–973 K and $V_3Ti_6O_7$ at 973–1073 K due to the reaction of dispersed

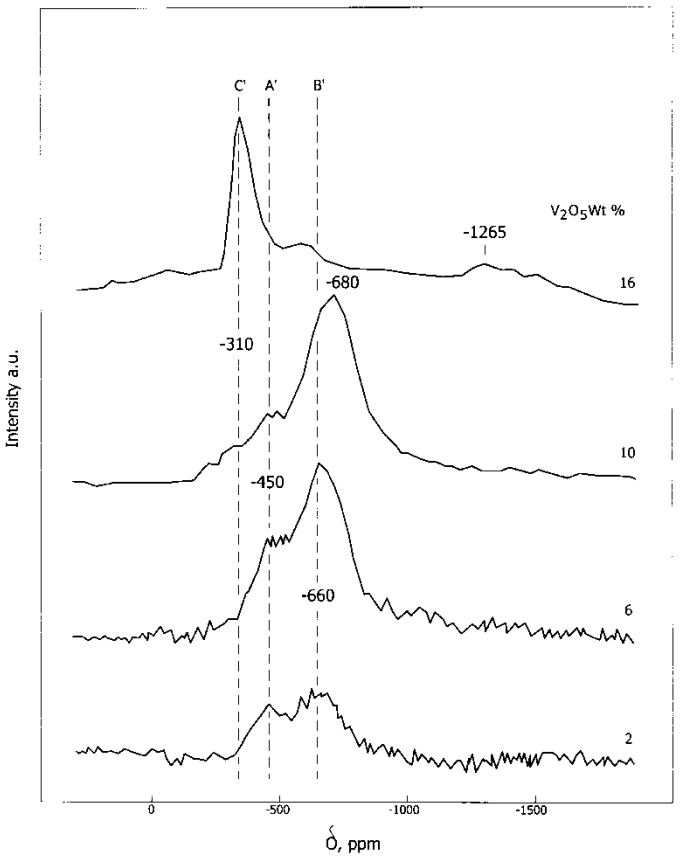


**Figure 7:** Solid-state $^{51}V$ NMR spectra of $V_2O_5/TiO_2$-$ZrO_2$ catalysts obtained after evacuation of the samples at 523 K for 2 h. Reproduced from Ref. 89 with permission from ACS.

vanadium oxide with $ZrO_2$ and $TiO_2$, respectively. The formed $V_3Ti_6O_7$ compound was decomposed into $V_2O_5$ and $TiO_2$ at 1173 K as confirmed from FTIR and $^{51}V$ NMR measurements. The IR spectroscopic studies of ammonia adsorption on $V_2O_5/TiO_2$-$ZrO_2$ catalysts revealed the presence of both Lewis and Brönsted acid sites (90). Therefore, the $V_2O_5/TiO_2$-$ZrO_2$ catalysts were employed for both Lewis and Brönsted acid-catalyzed reactions. The TEM-energy-dispersive spectrometer (EDX) techniques were utilized to understand the nanostructural evolution of $TiO_2$-$ZrO_2$ and $V_2O_5/TiO_2$-$ZrO_2$ samples calcined at various temperatures (85). The $TiO_2$-$ZrO_2$ binary oxide, when calcined at 773 K, was in a poorly crystalline state and its crystallinity increased with increasing calcination temperature. A layer structure with a lattice spacing of 2.87 Å due to the (111) plane of the $ZrTiO_4$ compound was clearly noted, indicating its formation at higher temperatures. The $V_2O_5/TiO_2$-$ZrO_2$ sample calcined at 773 K showed heterogeneity in the distribution of vanadium oxide particles on the surface. Two regions, one with a highly

dispersed vanadium oxide and the other one with an isolated $V_2O_5$, were identified. The same catalyst, when treated at 873 K and above, showed more surface heterogeneity. Three regions were observed for the $V_2O_5/TiO_2$-$ZrO_2$ sample calcined at 1073 K as shown in Fig. 8. The corresponding EDX analysis presented in Fig. 9 revealed that the compositions of these regions are different. In one region Ti and Zr predominate with equal distribution and in another region the titanium was abundant. The third region was dominated by zirconium oxide along with vanadium oxide. These observations clearly indicated that the formation of $ZrTiO_4$ and $ZrV_2O_7$ compounds along with $TiO_2$ as established from X-ray diffraction (XRD) and other techniques (83, 88, 89). Chang and Wang reported that the incorporation of $V_2O_5$ into $TiO_2$-$ZrO_2$ not only induces the formation of crystalline $ZrTiO_4$ at lower temperatures, but also enhances its crystallinity (11). Moreover, the higher acidity of ternary oxides with a $V_2O_5$ molar ratio above 0.25 was proposed to be due to a phase separation between $V_2O_5$ and $ZrTiO_4$.

The DRIFT spectra of out gassed $V_2O_5/TiO_2$-$ZrO_2$ catalysts in the skeletal region 1400–400 $cm^{-1}$ were investigated by Lakshmi et al. (18). The observed bands at 1020 and 860 $cm^{-1}$ were attributed to the stretching vibrations of V=O and V–O–V bonds, respectively. At lower vanadia loadings, due to the overlap with the broad IR bands, vibrations corresponding to the surface vanadia species were not observed. The information pertaining to the presence of monolayers and multilayers of vanadia on the support surface were achieved from IR overtone absorptions. In the case of $V_2O_5/TiO_2$-$ZrO_2$ catalysts the over tones observed at 2010 and 1972 $cm^{-1}$ correspond to the $V_2O_5$ agglomerates. The DRIFT studies were in perfect agreement with $^{51}V$ NMR studies suggesting the presence of $V_2O_5$ clusters for high vanadium containing samples (18).

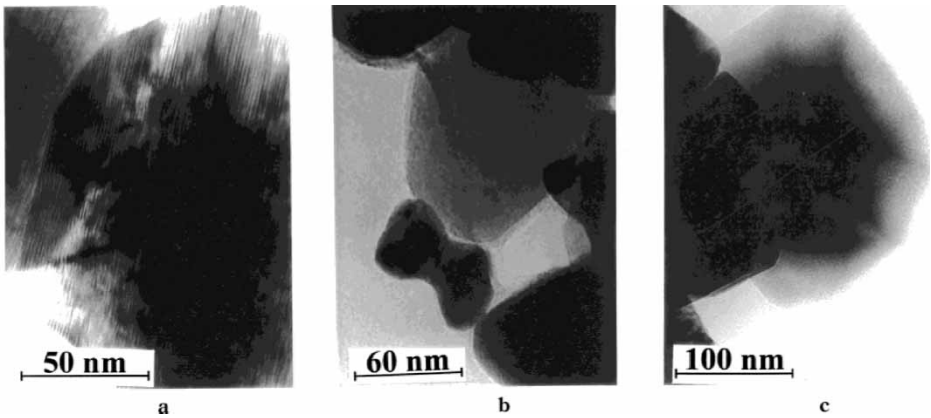


**Figure 8:** The TEM micrographs of $V_2O_5/TiO_2$-$ZrO_2$ catalyst calcined at 1073 K at different regions. Reproduced from Ref. 85 with permission from ACS.

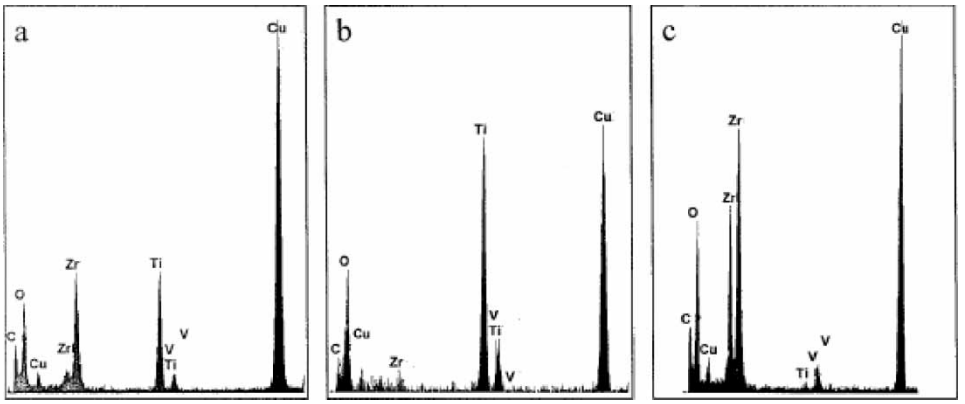


**Figure 9:** The EDX patterns of $V_2O_5/TiO_2$-$ZrO_2$ catalyst calcined at 1073 K corresponding to the TEM micrographs in Fig. 6. Reproduced from Ref. 85 with permission from ACS.

Raman spectroscopy technique is more sensitive to short-range order than is X-ray diffraction, and it can provide information on the intermediate crystallization of anatase or rutile as well as monoclinic zirconia before that of $TiZrO_4$. Knözinger and coworkers (34) have thoroughly investigated using Raman spectroscopy the structural characteristics of $MoO_3/TiO_2$, $MoO_3/ZrO_2$, and $MoO_3/TiO_2$-$ZrO_2$ catalysts obtained by both conventional wet impregnation and nonconventional solid-solid wetting methods. The Raman spectrum of the $TiO_2$-$ZrO_2$ sample calcined at 823 K, as shown in Fig. 10, contained broad bands at 144, 365, 585, and 764 $cm^{-1}$ presumably due to the characteristic bands of an amorphous material. The Raman measurements revealed, for all samples after treatment with moist oxygen, that the surface structures of $MoO_3$ are very similar to the structures of the catalysts prepared by incipient wetness impregnation method indicating a monolayer dispersion of molybdenum oxide on these supports. The structure of the dispersed species was identified as a polymeric surface molybdate species comparable to the hepta- or octa-molybdate anions. The nature of the surface molybdate species was independent of the preparation method. Dispersion starts during intense mixing, but thermal treatment is necessary to facilitate and finish the process. Raman spectra of $TiO_2$-$ZrO_2$ and $SO_4^{2-}$/$TiO_2$-$ZrO_2$ were investigated by Lai et al. (55). In the case of $TiO_2$-$ZrO_2$ sample, characteristic bands were observed at 170, 306, 338, 420, 519, 634, and 800 $cm^{-1}$, which are fairly in agreement with the Raman spectra of $TiZrO_4$ sample as reported by Andrianainarivelo et al. (72). The Raman spectra of the sulfated $TiO_2$-$ZrO_2$ samples were similar to those of non-sulfated samples, however, with increasing sulfuric acid strength significant changes in the spectra were observed with additional peaks pertaining to $TiOSO_4$ (55).

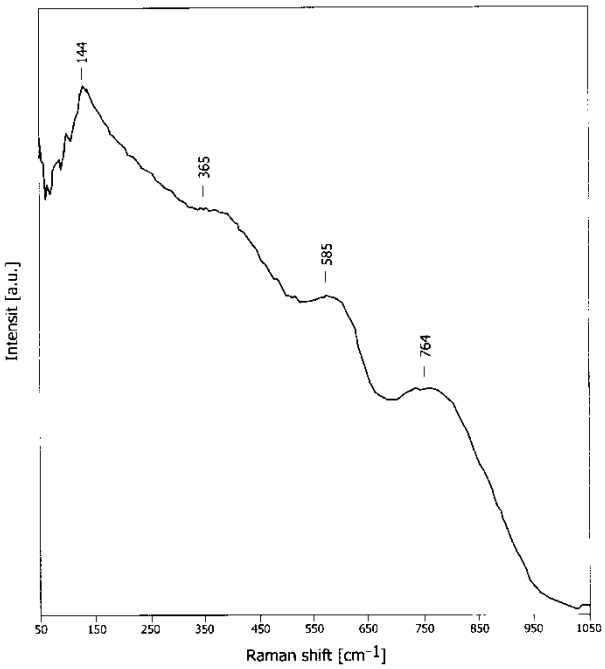


**Figure 10:** Laser Raman spectra of $TiO_2$-$ZrO_2$ calcined at 823 K. (From Ref. 34.)

The influence of $MoO_3$, $WO_x$, and $SO_4^{2-}$ on the physicochemical and catalytic properties of $TiO_2$-$ZrO_2$ were investigated by Reddy et al. (38, 39, 83, 84, 86, 119) and others (34, 37, 41, 42, 52, 54, 55). The XRD results revealed that up to monolayer coverage ($\sim$12 wt.%), the impregnated molybdenum oxide was in a highly dispersed form when calcined at 773 K (no characteristic peaks due to $MoO_3$). Only broad diffraction patterns due to amorphous $ZrTiO_4$ were observed (86). Oxygen chemisorption measurements performed under static conditions at low (195 K) and high (640 K) temperatures also revealed that the deposited $MoO_3$ was in a highly dispersed state (17). However, at higher calcination temperatures, beyond 873 K, the XRD peaks pertaining to $ZrMo_2O_8$ whose crystallinity also increased with increasing calcination temperature were observed. The XRD investigations revealed interesting information about the reactivity of dispersed vanadia and molybdena towards the $ZrTiO_4$ compound. It was found that the dispersed molybdena reacts preferably with the $ZrO_2$ portion of the $ZrTiO_4$ compound and forms a crystalline $ZrMo_2O_8$ phase. The corresponding $TiO_2$ from the $TiO_2$-$ZrO_2$ mixed oxide appears as crystalline anatase or rutile phase as shown in Eq. (5) (34, 83, 86):

$$ZrTiO_4 + 2MoO_3 \longrightarrow ZrMo_2O_8 + TiO_2(A/R) \quad (5)$$

However, the analogous reaction between dispersed vanadia and $ZrTiO_4$ resulted in the formation of $ZrV_2O_7$ and $TiO_2$-rutile phase as presented in Eq. (6.)

$$ZrTiO_4 + V_2O_5 \longrightarrow ZrV_2O_7 + TiO_2(R) \tag{6}$$

In the case of sulfate-ion impregnated $TiO_2$-$ZrO_2$ samples, in addition to $TiZrO_4$ a few extra lines due to the formation of $Ti_2(SO_4)_3$ and $Zr(SO_4)_2$ compounds were observed (38, 119). The formation of $Zr(WO_4)_2$ compound in addition to $ZrTiO_4$ was noted in the case of tungsten oxide–promoted catalysts (38, 119). Treatment of $TiO_2$-$ZrO_2$-mixed oxides with both sulfuric acid and aqueous ammonium sulfate led to a decrease in the specific surface areas. When acid of high concentration was employed, it penetrated into the bulk of the mixed oxides, thereby forming $TiOSO_4$. Thus a dissolution and recrystallization of different solid phases during the pretreatment were observed. This process was thought to be responsible for the diminution in the surface area of the treated samples. However, the addition of sulfate ions enhanced the acidity and catalytic activity of the $TiO_2$-$ZrO_2$ mixed oxides. Hence, a change in surface area simply cannot explain the change in activity of the mixed oxides. The sulfated $TiO_2$-$ZrO_2$ mixed oxide was found to be very active and selective towards the decomposition of dichlorodifluoromethane into carbon dioxide as elaborated in the next section of this paper.

The relative influence of $MoO_x$, $WO_x$, and $SO_4^{2-}$ on the surface properties of $TiO_2$-$ZrO_2$ was investigated by XPS technique (119). The XPS binding energies of Zr $2p_{3/2}$ and Ti $2p_{3/2}$ peaks were shifted towards higher energies for the sulfated samples. Apparently, the inductive effect of impregnated $SO_4^{2-}$ ions enhances acidity at the metal sites causing them to exhibit superacidity. This superacidity is of the Lewis type. However, in the presence of water, the catalyst surface gets hydroxylated and exhibits Brönsted acidity. The enhanced positive charge on the metal center also induces high acid strength to the nearby Brönsted acid sites (38, 119). The mixed oxides with $M-O-M^1$ bonds were found to be acidic in nature due to the charge imbalance of the metal ions. The relative dispersion and nature of the dispersed molybdenum oxide on various mixed oxides, namely $TiO_2$-$SiO_2$, $TiO_2$-$Al_2O_3$, $TiO_2$-$ZrO_2$, and $SiO_2$-$TiO_2$-$ZrO_2$ were systematically investigated by X-ray photoelectron spectrometry and other techniques by Reddy et al. (83). These studies revealed that at low loadings molybdena reacts strongly by forming bidentate species as shown in Fig. 11 with a pair of adjacent surface hydroxyl groups of the support. However, at higher loadings (above monolayer coverage) multilayer and three-dimensional growth of molybdate crystals were postulated in line with the literature reports (120, 121). Thus various characterization results revealed that the $TiO_2$-$ZrO_2$ mixed oxide is highly promising for the dispersion of various transition metal oxides and sulfate ions for exploiting them for different catalytic applications.

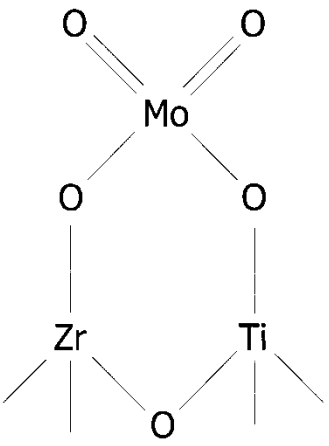


**Figure 11:** Schematic representation of dispersed molybdena bi-dentate species over $TiO_2$-$ZrO_2$ support. (From Ref. 83.)

## 4. CATALYTIC APPLICATIONS

### 4.1 Dehydrogenation

The catalytic dehydrogenation of ethylbenzene is of industrial importance in the manufacture of styrene. The feasibility of carrying out this reaction over $TiO_2$-$ZrO_2$ was first reported in 1963 (122). Wang and coworkers have extensively studied various dehydrogenation reactions over $TiO_2$-$ZrO_2$ mixed oxides (8–10). In their work, a series of $TiO_2$-$ZrO_2$ catalysts with different molar ratios were evaluated for the oxidative dehydrogenation of ethylbenzene and ethylcyclohexane. A good correlation was observed between the activity and the surface acid–base properties of the catalysts. A high catalytic activity was noted when the two components, $TiO_2$ and $ZrO_2$, were present at a compatible amount (equimolar ratio). The selectivity of styrene increased monotonously with increase in $TiO_2$ content. The activity was poisoned not only by $K_2O$ but also by $B_2O_3$ indicating that the active sites involved are both acidic and basic. The activity results strongly suggested that the $TiO_2$-$ZrO_2$ is an acid-base bifunctional catalyst. Thus a concerted two-center mechanism was proposed, wherein zirconium ion acts as a Lewis acid site and titanium ion as a base site (8). This study was further extended by subjecting the $TiO_2$-$ZrO_2$ (1 : 1) mixed oxides to high thermal treatments and the observed high activity was attributed to the formation of $ZrTiO_4$ phase (9). It was concluded from their investigations that the formation of $ZrTiO_4$ compound and an increase in the amounts of acid-base sites are the major factors affecting the catalytic activity towards styrene production. The $TiO_2$ and $ZrO_2$ alone are impractical as catalysts for dehydrogenation of ethylbenzene. It was also

further postulated that ethylbenzene and ethylcyclohexane are initially activated by the acid sites of the binary oxides and then undergo the dehydrogenation reaction over the basic sites. The activities of both ethylbenzene and ethylcyclohexane dehydrogenations were compared. The relatively stronger acid sites, instead of the moderate ones, which are suitable for ethylbenzene dehydrogenation, are required for ethylcyclohexane dehydrogenation too (8–10).

Chang and Wang investigated the isomerization and dehydrogenation of cyclohexane over $TiO_2$-$ZrO_2$-$V_2O_5$ ternary oxides prepared by the coprecipitation method (11). The $TiO_2/ZrO_2$ (1 : 1) binary oxide alone was found to be impractical for dehydrogenation of cyclohexane. However, the $TiO_2$-$ZrO_2$-$V_2O_5$ ternary oxide was observed to be more effective and a maximum activity was noted at a $V_2O_5$ molar ratio of 0.1. A speculative stepwise two-center mechanism was proposed. The abstraction of a hydride ion by an acid site to form cyclohexyl carbenium ion intermediate appears to be the slow rate-determining step, whereas the removal of proton by basic sites is the fast step. A relationship between the skeletal isomerization of hydrocarbons and concentration of stronger acid sites of catalysts is a generally accepted fact. To elucidate the role of acidic and basic sites in the dehydrogenation of cyclohexane, $K_2O$, and $B_2O_3$ were also incorporated into the $TiO_2$-$ZrO_2$-$V_2O_5$ catalysts by wet impregnation method. Based on these results, it was concluded that the acidic sites of $TiO_2$-$ZrO_2$-$V_2O_5$ play an important role in the dehydrogenation of cyclohexane (11).

Synthesis of isobutyraldehyde over $V_2O_5/TiO_2$-$ZrO_2$ mixed oxides from a mixture of methanol and ethanol (mole ratio 2 : 1 without or with 50 % v/v water) in one step was reported by Reddy et al. (21, 22). Isobutyraldehyde and its derivatives (e.g., isobutanol, isobutyric acid, and neopentyl glycol) are very useful chemical feedstocks in the plastic industry. Normally isobutyraldehyde is produced as a by-product in the OXO process (hydroformylation of propene with CO and $H_2$). However, this is an energy consuming process. The single-step reaction between methanol and ethanol is an interesting reaction from the point of view of ethanol utilization and is also a useful alternative to the conventional hydroformylation process.

## 4.2 Decomposition of Chlorofluoro Carbons (CFCs)

Tajima et al. (53, 54) investigated the decomposition of chlorofluorocarbons (CFC 113) in the presence of water over a variety of solid acid catalysts. The $TiO_2$-$ZrO_2$ was found to exhibit its highest activity and longest life among various catalysts examined. The catalytic activity of $TiO_2$-$ZrO_2$ also increased with an increase in the content of $TiO_2$. The mixed oxide containing 58 mole % $TiO_2$ exhibited highest activity. Interestingly, crystallinity of the $TiZrO_4$ phase was also maximum for the 58 mole % $TiO_2$-containing sample. Therefore, it was

proposed that the crystallinity of $TiZrO_4$ influences the catalytic activity of decomposition of CFC 113 (1,1,2-Trichloro-1,2,2-trifluoroethane). However, the catalyst was deactivated gradually due to the removal of Ti atoms from the $TiO_2$-$ZrO_2$ binary oxide (confirmed with XPS). A good relationship was observed between the activity and bond energy of C-Cl in the compounds of chlorofluorocarbons and hydrochlorocarbons, suggesting that the rate-controlling step is the cleavage of the C-Cl bond. To overcome the deactivation crisis the same authors investigated the role of metal oxides on the $TiO_2$-$ZrO_2$ support. The tungsten oxide loaded $TiO_2$-$ZrO_2$ (W/TZ) was found to exhibit the highest activity and longest life among various catalyst combinations examined (V, Cr, Mn, Fe, Co, Ni, Mo, and Pd). The activity of W/$TiO_2$-$ZrO_2$ catalyst was also related to the amount of W loading. However, the decomposition of CFC-113 over W/$TiO_2$-$ZrO_2$ produced an undesirable side product, CO, in an amount equal to $CO_2$. It was proved from other experiments that a Pd/$TiO_2$-$ZrO_2$ catalyst selectively oxidizes CO to $CO_2$. Therefore, a combination catalyst obtained by mechanical mixing of Pd/$TiO_2$-$ZrO_2$ and W/$TiO_2$-$ZrO_2$ was employed to decompose the CFC-113 to produce $CO_2$ selectivity.

Catalytic hydrolysis of dichlorodifluoromethane (CFC-12) on unpromoted and sulfate ion promoted $TiO_2$-$ZrO_2$ mixed oxide catalysts was investigated by Lai et al. (52, 55). Sulfated catalysts exhibited enhanced activity and the catalytic activity also increased with an increase in the acid strength of impregnated sulfuric acid. The sulfated catalyst obtained by treatment with 96% sulfuric acid exhibited maximum activity, capable of complete conversion of CFC-12 with 100% selectivity to $CO_2$ at 553 K. These authors further (52) investigated the influence of gold nanoparticles on the sulfated $TiO_2$-$ZrO_2$ catalyst for CO oxidation during catalytic decomposition of chlorodifluoromethane (HCFC-22). The gold-promoted sulfated $TiO_2$-$ZrO_2$ catalyst was found to be active for the oxidation of carbon monoxide at room temperature in the presence of water vapor. However, the selectivity of the catalyst to $CO_2$ during the decomposition of HCFC-22 in the presence of water vapor increased marginally. Apparently, the HF and HCl formed during the hydrolysis of HCFC-22 deactivate the gold nanoparticles. Therefore, it was concluded that the addition of gold enhances the selectivity towards $CO_2$ by a smaller extent.

## 4.3a Epoxides to Alcohols

The isomerization of 1-methylcyclohexene oxide and cyclohexene oxide at 381 K over $TiO_2$-$ZrO_2$ of various compositions predominantly provided allyl alcohol with endo double bond 2-methyl-2-cyclohexene-1-ol and 2-cyclohexen-1-ol, respectively (5, 6). The catalytic activity was correlated well with both

the acidity and basicity of the catalysts. It is a known fact that acid sites are active for the selective formation of ketone and basic sites are almost inactive for the isomerization of 1-methylcyclohexene oxide or cyclohexene oxide. Therefore, the formation of allyl alcohol over $TiO_2$-$ZrO_2$ indicates the involvement of both acidic and basic sites. Hence, an acid-base bifunctional mechanism was utilized to explain the previous phenomenon. Subsequently, it was concluded that the epoxide is adsorbed on both acidic and basic sites and allyl alcohol is formed when opening of both the epoxide ring and hydrogen abstraction took place simultaneously, while ketone is formed when the former precedes the latter. Tanabe et al. (7) also investigated the rearrangement of 2-carene oxide over $TiO_2$-$ZrO_2$ (1 : 1) catalyst that resulted in an allyl alcohol [cis-2, 8 (9)-*p*-menthadiene-1-ol].

## 4.3b Synthesis of ε-Caprolactam

The production of ε-caprolactam through Beckmann rearrangement of cyclohexanone oxime is commercially viable, as it is the precursor to nylon-6. Mao et al. (14, 15) investigated the previous reaction over various boria-impregnated binary oxides. The performance of these catalysts was found to be sensitive to the dispersion of boria and nature of the support. Supports which exhibit both acidic and basic characteristics exhibited better catalytic properties for this reaction. Among various catalysts investigated, the $B_2O_3$/$TiO_2$-$ZrO_2$ exhibited better activity and selectivity for the rearrangement of ε-caprolactam. Among various $TiO_2$-$ZrO_2$ mixed oxides investigated, the one having equimolar composition of $TiO_2$ and $ZrO_2$ exhibited highest activity. Interestingly, the ε-caprolactam yield increased with increasing boria loading up to 12 wt.%. Both pore size distribution and acid strength of $B_2O_3$/$TiO_2$-$ZrO_2$ catalysts were thought to play an important role in the selective formation of the lactam. Conversion of oxime also increased with increase in the reaction temperature, however, up to 573 K. The acid sites of medium strength on the surface of the $B_2O_3$/$TiO_2$-$ZrO_2$ catalyst play an important role in the selective formation of the lactam. As discussed earlier, the $TiO_2$-$ZrO_2$ mixed oxide possesses both acidic and basic sites. Supporting boria over $TiO_2$-$ZrO_2$ reduces the basic sites in the system and, thereby, brings the conversion of oxime into lactam (14, 15).

## 4.4a Partial Oxidation

Partial oxidation of methanol and ethanol over $TiO_2$-$ZrO_2$ and $V_2O_5$/$TiO_2$-$ZrO_2$ catalysts was investigated by Reddy et al. (16, 17) and Lakshmi et al. (18), respectively. Lakshmi et al. (18) evaluated the catalytic properties of various mixed oxide–supported vanadium oxide catalysts for the model reaction–ethanol partial oxidation. It was observed that the ethanol partial oxidation

rates of various catalysts increased with increase in reaction temperature. Further, the partial oxidation rates of $V/TiO_2$-$SiO_2$, $V/TiO_2$-$Al_2O_3$, and $V/TiO_2$-$ZrO_2$ catalysts were not much different from one another indicating that a similar kind of reactivity exists in all three series of catalysts. The overlap of reaction rates in each series of catalysts was attributed to the structure-insensitive nature of ethanol partial oxidation. With in the $V/TiO_2$-$ZrO_2$ series of catalysts, the reaction rates were in the order of $V/TiO_2 > V/ZrO_2 = V/TiO_2$-$ZrO_2$. A total selectivity to acetaldehyde was observed only at low reaction temperatures. This study indicated that certain optimum vanadia loading is required for the best catalytic activity (18). Partial oxidation of methanol to formaldehyde was selected as a probe reaction by Reddy et al. (16, 17) for evaluating the relative reactivities of various $V_2O_5/TiO_2$-$ZrO_2$ catalysts. These studies were carried out at low temperatures ($\sim$448 K) in order to minimize the formation of high-order products such as dimethoxy methane, methyl formate, etc. The conversion of methanol increased with vanadia loading up to 12 wt.% $V_2O_5$. This study further established a direct relationship between oxygen uptake capacity (a measure of vanadia dispersion) and total conversion of methanol at all vanadia loadings (16). Feil et al. (123) and Chung et al. (124) envisaged a reaction mechanism for the oxidation of methanol, which involves the dissociative adsorption of $CH_3OH$ ($CH_3O^- + H^-$) to form surface methoxide ions. The next step in the catalytic cycle, which is also widely accepted (125), is the abstraction of a methyl hydrogen by the surface oxygen, followed by a rapid intramolecular rearrangement and desorption of formaldehyde and other products. Oxygen uptake and methanol oxidation activity trends observed on various samples indicated that coordinatively unsaturated V-oxide sites are the plausible locations for the initial dissociative adsorption of methanol, where oxygen too adsorbs selectively on these sites. This study indicates that oxygen vacancies are the active sites and the methoxy species are the reaction intermediates. Generally, the active sites (oxygen vacancies) are greatly influenced by geometric and electronic factors and are responsible for the formation of different resultant compounds. Formaldehyde and CO were thought to be produced mainly from methoxy species adsorbed on terminal oxygen vacancy (M=O) sites and the bridged oxygen vacancy sites are responsible for the formation of high order products (126). During the reaction, the terminal oxygen vacancies are more abundant than are the bridged oxygen vacancies, because the bridged oxygen vacancy site is reoxidized more easily than is the terminal oxygen vacancy site (126). These comprehensive investigations revealed that the $V_2O_5/TiO_2$-$ZrO_2$ catalysts exhibit more activity and selectivity than do the corresponding single oxide–supported catalysts. Another important observation made from these investigations was that the monolayer catalysts are more active than the multilayer, microcrystalline, or bulk vanadium oxide catalysts.

## 4.4b Deep Oxidation

Among various metal catalysts that have been reported for soot oxidation, Pt exhibits a high level of catalytic activity (127–129). In order to meet the stringent environmental regulations, design of Pt catalysts over various mixed oxides was undertaken and their efficiency was also evaluated under synthetic gas and practical diesel exhaust conditions. With respect to the reaction mechanism, Pt promotes soot oxidation indirectly; that is, by catalyzing oxidation of the NO present in the exhaust gas to $NO_2$, which subsequently oxidizes soot to $CO_2$. Furthermore, it was found that the $H_2SO_4$, produced by the oxidation of $SO_2$ on the Pt surface, catalyzes the oxidation reaction of carbon by $NO_2$. In this reaction system, the catalytic activity for carbon oxidation was drastically increased when the $SO_2$ content in the reactant gas reached 8 ppm. These authors were successful in devising new catalytic systems, which could even operate with a 2 ppm level of sulfur. However, the $Pt/TiO_2$-$ZrO_2$ catalysts were found to be somewhat less effective than was $Pt/TiO_2$-$SiO_2$ (25).

Lin et al. recently reported $Pd/TiO_2$-$ZrO_2$ as a novel catalyst for methane combustion at low temperatures (26). The $Pd/TiO_2$-$ZrO_2$ catalyst exhibited much higher activity than did $Pd/TiO_2$ and $Pd/ZrO_2$. The TPR and $^{18}O$-isotope exchange measurements demonstrated that the excellent activity of $Pd/TiO_2$-$ZrO_2$ is due to its high oxygen mobility and moderate reducibility.

## 4.5a Hydrogenation

Vapor-phase hydrogenation of naphthalene over various supported Pt catalysts was investigated by Lu et al. (27). The experimental results indicated that the catalytic activity strongly depends on the nature of support and the prereduction temperature. Among various supported Pt catalysts examined the one supported on $TiO_2$-$ZrO_2$ (1 : 1) exhibited the highest activity. This work was mainly aimed at understanding the electronic effect of Pt on $TiO_2$-$ZrO_2$ with various Ti/Zr ratios and other mixed oxides. Significant interaction between the metal and the support was noted in the case of $Pt/TiO_2$-$ZrO_2$ catalysts. Vannice and co-authors (130–132) conclude from their systematic studies on the hydrogenation of benzene that the use of acidic supports enhances the rate of hydrogenation. As reported by Wu and coworkers (8, 9), the acidity of $TiO_2$-$ZrO_2$ reaches its maximum at 50 mole % $ZrO_2$. The hydrogenation activity results indicated that an increase in the acidity of the support enhances the hydrogenation activity, thereby allowing more aromatic reactant to be adsorbed. Therefore, the $Pt/TiO_2$-$ZrO_2$ (1 : 1 ratio) catalyst exhibited maximum hydrogenation ability.

## 4.5b Hydrotreating

Titania-zirconia mixed oxide aerogels of varying stoichiometries obtained by supercritical fluid extraction analogy (SCF) were employed as supports for Ni-Mo catalysts for hydroprocessing [hydrodesulfurization (HDS), hydrodenitrogenation (HDN), hydrodeoxygenation (HDO), hydrodemetallation (HDM), etc.] of gas oil in a pilot plant scale reactor (32). The high $ZrO_2$-containing materials were found to be unstable under reaction conditions and were nearly inactive. In contrast, the high $TiO_2$-containing mixed oxides were more active when compared to the corresponding single oxide and conventional $A1_2O_3$ supported catalysts. This particular improvement was attributed to the properties inherent to the SCF-prepared samples, thus emphasizing the significance of surface acidity to hydrotreating activity. The SCF-obtained $TiO_2$-$ZrO_2$ supports exhibited high specific surface area and high surface acidity. After super critical extraction and calcination at 773 K, the mixed oxide aerogels possessed higher surface acidity than did the pure components, as measured by Hammett indicators, and were poorly crystalline, both indicative of a strong interaction between the two component oxides. This interaction helps to stabilize the mixed oxides and provides an underlying reason for the observed high specific high surface area and high surface acidity. However, the supports obtained by the SCF method were not highly stable under the reaction conditions, suffered significant loss in the surface area, and an increase in the crystallinity after exposure to hydrotreating conditions. High $ZrO_2$ content supports were exceptionally prone to collapse, forming low surface area materials having almost no catalytic activity. The high $TiO_2$ content SCF materials exhibited enhanced HDN activities and selectivities, and suffered a partial collapse (32). Maity et al. also reported a better hydrotreating functionality over a 12 wt.% $Mo/TiO_2$-$ZrO_2$ catalyst having 65 : 35 mole ratio of titania and zirconia (33). Recently, a wide pore $TiO_2$-$ZrO_2$ obtained by a low temperature sol-gel technique followed by solvo-treatment was employed for hydrodesulfurization of dibenzothiophene after impregnating it with $MoS_2$ (31). This catalyst was found to exhibit excellent catalytic activity and seems to be a promising support for new generation hydrotreating catalysts.

## 4.6 Organic Transformations

A variety of aromatic and aliphatic aldehydes were converted into their 1,1-diacetates over molybdate-promoted $TiO_2$-$ZrO_2$ solid acid catalysts under solvent-free conditions (38, 39). Diacetates are potential aldehyde protecting groups and important precursors in the synthesis of dienes for Diels-Alder reactions (133). The main advantage in diacetalization of aldehydes is that the diacetates formed are quite stable in neutral, acidic, and basic media (133). The sulfated $ZrO_2$ and $TiO_2$-$ZrO_2$ catalysts exhibited better activity

and product selectivity for various organic synthesis and transformation reactions in the liquid phase under very mild reaction conditions (38, 39, 134–136). However, the sulfated catalysts were deactivated rapidly and tended to leach $H_2S$ and $SO_x$ during preparation (in the presence of $H_2$ and air treatment) and catalytic runs. Recent investigations revealed that tungstate- or molybdate-doped catalysts are the best alternatives in reactions requiring stronger acid sites (137–139). The promoted $TiO_2$-$ZrO_2$ solid acid catalysts are expected to find numerous applications in synthetic organic chemistry (38). The relationship between acidic properties of $NiSO_4/TiO_2$-$ZrO_2$ and their catalytic activity for acid-catalyzed reactions was investigated by Sohn et al. (41) by using cumene dealkylation as a test reaction. The existence of both Brönsted and Lewis acid sites on $NiSO_4/TiO_2$-$ZrO_2$ catalysts was established by in-situ ammonia adsorption by IR spectroscopy.

## 4.7 $NO_x$ Abatement

Air pollution by nitrogen oxides ($NO_x$) emitted from mobile and stationary sources is a serious environmental problem still attracting considerable attention both in academia and on the industrial front. The selective catalytic reduction of $NO_x$ with hydrocarbons or oxygenated hydrocarbons (HC-SCR) in the presence of oxygen has gained much focus recently. The catalytic performance of metal (Ag/In/Pt) impregnated $TiO_2$-$ZrO_2$ for the selective reduction of NO with propene, 2-propanol, acetone, and methane was investigated by Haneda et al. (44, 45, 47, 48), Machida et al. (43, 49), and Mariscal et al. (46). The addition of silver to $TiO_2$-$ZrO_2$ caused a dramatic enhancement of NO reduction activity with propene (45). The influence of silver additive was explained by the assumption that silver promotes the reaction of $NO_2$ with propene to form a partially oxidized hydrocarbon, which is the rate-determining step. Oxygen-containing compounds such as 2-propanol and acetone were also found to be good reductants for NO reduction over $Ag/TiO_2$-$ZrO_2$ catalysts. Further, the presence of water vapor significantly enhanced the NO reduction activity of the $Ag/TiO_2$-$ZrO_2$ catalysts with these reductants. Apparently, the water vapor accelerates the reduction of NO by suppressing the undesirable oxidation of the reductants by $O_2$ (45). Very similar results were obtained for the catalytic reduction of NO with propene over $In/TiO_2$-$ZrO_2$ catalysts (47). From FT-IR measurements under static conditions, organic nitro- (R-$NO_2$), nitrite- (R-ONO), inorganic $NO_3^-$, carbonate, formate, and acetate species were detected when $TiO_2$-$ZrO_2$ or $Ag/TiO_2$-$ZrO_2$ was exposed to a gas mixture of $NO + C_3H_6 + O_2$ at room temperature. In the case of $Ag/TiO_2$-$ZrO_2$, an intense IR band assigned to isocyanate (-NCO) species was observed after being exposed to $NO + C_3H_6 + O_2$ and evacuated at temperatures above 573 K. However, under dynamic conditions the isocyanate band was detected on $TiO_2$-$ZrO_2$ but not on $Ag/TiO_2$-$ZrO_2$. A reaction

mechanism for the selective reduction of NO with propene over $Ag/TiO_2$-$ZrO_2$ has been proposed as shown in Fig. 12. According to this scheme, propene initially reacts with $NO_2$ and/or $NO_3^-$, which are formed from NO and $O_2$ on the acid sites of $Ag/TiO_2$-$ZrO_2$, resulting in the formation of organic nitro- and nitrite- compounds. These compounds are then converted into isocyanate and cyanide species on Ag sites. Finally, the isocyanate species is reduced to $N_2$ by the reaction with $NO_2$. Low temperature catalytic $NO_x$-$H_2$-$O_2$ reaction over $Pt/TiO_2$-$ZrO_2$ was investigated by Machida et al. (43). The reaction was performed in a stream of NO (0.08 vol.%)-$H_2$ (0.08–0.56 vol.%)-$O_2$ (10 vol.%) at low temperatures (<273 K). The NO conversion to $N_2/N_2O$ occurred at >0.08 vol.% $H_2$, and the selectivity to $N_2$ increased with increasing $H_2$ concentration. In-situ DRIFTS measurements suggested that the high selectivity in this temperature range is closely related to a stoichiometric reaction between $H_2$ and NO oxidatively adsorbed as nitrate ($NO_3^-$) species. This study also thrown light on the role of catalyst pretreatment on the NO reduction activity, i.e., a reduced catalyst exhibited much higher activity than did an oxidized catalyst. The effect of pretreatment was consistent with the reactivity of nitrate adsorbates formed on Pt surface towards $H_2$. Subsequently, Machida et al. (49) reported a dual-bed lean de$NO_x$ catalyst system for NO-$H_2$-$O_2$ reaction and subsequent $N_2O$ decomposition. The serial dual-bed catalytic system consisted of $Pt/TiO_2$-$ZrO_2$ in the first bed and $Pd/Al_2O_3$ in the second one. In the first bed at ≤273 K, ca. 80%–90% of NO was converted into $N_2/N_2O$ by selective reduction with $H_2$. Further, almost all the $N_2O$ thus formed in the first bed was successfully decomposed into $N_2/O_2$ in the second bed at 673 K. The NO reduction with $CH_4$ over $Pt/TiO_2$-$ZrO_2$ was investigated by Marsical et al. (46). The $TiO_2$-$ZrO_2$ support was particularly chosen as it displays unusual acidic properties and very high

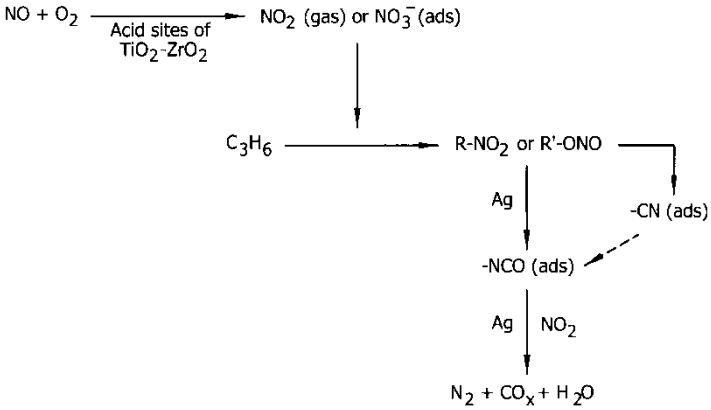


**Figure 12:** Schematic representation of proposed reaction mechanism for the selective reduction of NO with propene over $Ag/TiO_2$-$ZrO_2$. (From Ref. 44.)

thermal resistance. These properties are of paramount importance because the activation of the C-H bond of $CH_4$ occurs at rather high temperatures. The DRIFT spectra of CO adsorbed on the $Pt/TiO_2$-$ZrO_2$ catalysts revealed that an SMSI state develops in the Ti-rich oxide-supported platinum catalysts. However, no shift in the binding energy of Pt $4f_{7/2}$ level was observed from XPS. The DRIFT spectra of the catalysts under the $NO + O_2$ co-adsorption revealed the appearance of bands due to nitrite/nitrate species on the surface of the catalysts, whose intensity being reached maximum in the case of $Pt/TiO_2$-$ZrO_2$ (1 : 1 ratio). In the absence of oxygen in the feed stream, the $NO + CH_4$ reactions showed isocyano species in the DRIFT spectra, formed at the Pt-support interface.

## 4.8 Photo Catalytic Applications

The $TiO_2$ is a well-known photo catalyst (140–142). To enhance the quantum efficiency of $TiO_2$, modifications are normally introduced into the crystalline matrix by selective doping of foreign metal ions. Binary metal oxides of titania could enhance the photo catalytic degradation rates of some organic compounds in the environment, such as salicylic acid in water and ethylene in air. Navio et al. (61) investigated the photo catalytic oxidation of 1,4-pentanediol in oxygen atmosphere over UV-illuminated $ZrTiO_4$ particles in acetonitrile suspensions. The temporal course of the photo-oxidation of this diol was monitored by gas chromatography-mass spectrometry (GC-MS). A practically total regiochemical preference for oxidation of the primary hydroxyl group in 1,4-pentanediol was observed, with 4-hydroxypentanoic acid and its $\gamma$-lactone derivative as the sole products. Colon et al. (62) synthesized two different $ZrO_2$-$TiO_2$ photo catalysts by precipitating from $ZrOCl_2 \cdot 8H_2O$ precursor along with preformed $TiO_2$ (Degussa P25 and Hombikat UV-100) and investigated photo oxidation of salicylic acid and photo reduction of Cr(VI). It was observed from this study that the $ZrO_2$-$TiO_2$ is a good alternative to commercial $TiO_2$ (Degussa P25 and Hombikat UV-100) for the previously mentioned reactions. Yu et al. (58) and Zorn et al. (57) investigated the photo catalytic oxidation/degradation (PCO/PCD) of acetone over $Ti_{1-x}Zr_xO_2$ solid solutions and $TiO_2/ZrO_2$ thin films, respectively. The increased activity for the oxidation of acetone in air exhibited by $Ti_{1-x}Zr_xO_2$ solid solutions other than pure $TiO_2$ was attributed to changes in the lattice parameters caused by zirconium substitution. It was proposed that the lattice $O^{2-}$ and $O^-$ species ionosorbed on the surface are responsible for the increased photo activity. Anderson and coworkers (56) also performed the photo oxidation of ethylene in water over $TiO_2/ZrO_2$ mixed oxide thin films in the presence of microwave irradiation. The typical microwave photo catalytic reactor assembly employed for the photo catalytic reaction consisted of a fluorescent lamp located in the microwave field, the bulb emitted UV light

without electric power, i.e., on irradiation with microwaves. This process is called microwave plasma lighting. The photo catalytic activities of $TiO_2$-$ZrO_2$ mixed oxides, $TiO_2/ZrO_2$ thin films, and $ZrTiO_4$ (zirconium titanates) were found to depend on the type of photochemical reaction being carried out. Navio et al. (60) performed the photoconductivity measurements to correlate the photo electronic properties of $ZrTiO_4$ with its photo catalytic activity. It was observed that $ZrTiO_4$ becomes a photoconductor on exposure to near-UV illumination due to electron-hole pair formation. The $ZrTiO_4$ was found to be photoactive for isopropanol oxidation. Navio et al. (63) further employed the laser flash photolysis technique to estimate the inherent photocatalytic activity of $ZrTiO_4$ and its parent oxides, $ZrO_2$ and $TiO_2$. The reduction of methyl viologen ($MV^{2+}$) by conduction-band electrons of $ZrTiO_4$, $ZrO_2$, and $TiO_2$ was investigated and observed some correlations.

Novel $TiO_2/Zr_xTi_{1-x}O_2$ composite photocatalytic films, for the first time, were reported by Lu and co-workers by employing sol-gel technique (59). The structural characteristics of these composite films were investigated by employing AFM technique as described in the previous section. The photocatalytic activity and stability of these films were found to be greater than that of pure $TiO_2$ films. This was attributed to the higher separation efficiency of the photo-generated carriers and larger surface area by the introduction of intermediate layers of $Zr_xTi_{1-x}O_2$ in the composite films. According to these authors, introduction of $Zr_xTi_{1-x}O_2$ intermediate layers causes major changes. First, the composite films have smaller crystallite size, which can suppress the electron-hole recombination and improve the separation efficiency because the time needed to transfer the carriers from interior to surface is shorter. Secondly, the larger surface roughness of the composite film helps to improve the photo activity because it can increase the effective surface area of the photocatalytic reaction. Further, the introduction of an intermediate layer could optimize the interface structure because of the discrepancy of the crystal lattices between $Zr_xTi_{1-x}O_2$ and $TiO_2$. That is to say, the discrepancy can induce deformation of the interface structure, which can reduce the recombination rate and improve the separation efficiency of the carriers.

## 4.9 Other Applications

The $ZrTiO_4$ thin films were fabricated from metal oxide precursor solution by dip-coating method and tested as hydrocarbon gas sensors (66). These thin films were found to exhibit good response and sensitivity for propane and methane gases. The $TiO_2$-$ZrO_2$ catalysts in combination with $Y_2O_3$ were prepared in varying proportions ranging from 0 to 100 mol % of oxide components and were investigated for their catalytic performance for methanol hydrosulfurization (30). A high yttria content favored selectivity to methanethiol, while dimethyl-sulfide formation was noted at low loadings. A green

process of ozone-mediated nitration of chloro-benzene with $NO_2$ over $SO_4^{2-}$/$TiO_2$-$ZrO_2$ catalysts was reported by Cheng et al. (37). These catalysts exhibited excellent para-selectivity at 273 K. *p*-Mentha-1,8-dien-4-ol, useful as an intermediate for perfumes, was prepared in good yields by isomerization of spirooxirane over $TiO_2$-$ZrO_2$ catalysts in the liquid phase using toluene as the solvent at 373 K (35). Also preparation of chlorobenzene from polychloro compounds and benzene over titania-zirconia catalysts at 673 K was claimed recently (36).

## 5. CONCLUDING REMARKS

One of the aims of this review was to illustrate the significance of titania-zirconia mixed oxides as catalysts and catalyst supports as employed for a wide variety of catalytic applications both in the liquid and gaseous phases. In particular, we were interested in bringing together the entire literature pertaining to these mixed oxides with catalysis perspective. As discussed, these mixed oxides represent an interesting class of catalysts and catalyst supports, which have been widely employed in oxidation catalysis, acid-base catalysis, and photo catalysis. The intimate interaction between $TiO_2$ and $ZrO_2$ has been shown to result in new structural characteristics and reactivity properties. The degree of interaction largely depends on the preparation method and synthesis conditions. These materials are going to find numerous applications in the coming years both as catalysts and catalyst carriers.

## ACKNOWLEDGMENT

Support from the Department of Science and Technology, New Delhi, is gratefully acknowledged (SERC Scheme: SP/S1/H-20/98).

## REFERENCES

[1] Kung, H.H. (1989) *Transition Metal Oxides: Surface Chemistry and Catalysis*; Stud. Surf. Sci. Catal., Elsevier: Amsterdam; Vol. 45, 1–277.

[2] Henrich, V.E. and Cox, P.A. (1994) *The Surface Science of Metal Oxides*; Cambridge University Press: Cambridge, UK.

[3] Noguera, C. (1996) *Physics and Chemistry at Oxide Surface*; Cambridge University Press: Cambridge, UK.

[4] Reddy, B.M. (In press) Redox Properties of Metal Oxides. In *Metal Oxides: Chemistry and Applications*; Fierro, J.L.G., ed.; Marcel Dekker Inc.

[5] Arata, A., Akutagawa, S., and Tanabe, K. (1976) *Bull. Chem. Soc. Jpn.*, 49: 390.

[6] Arata, A. and Tanabe, K. (1980) *Bull. Chem. Soc. Jpn.*, 53: 299.

[7] Tanabe, K. and Yamaguchi, T. (1994) *Catal. Today*, 20: 185.

[8] Wang, I., Chang, W.F., Shiau, R.J., Wu, J.C., and Chung, C.C. (1983) *J. Catal.*, 83: 428.

[9] Wu, J.C., Chung, C.C., Ay, C.L., and Wang, I. (1984) *J. Catal.*, 87: 98.

[10] Wang, I., Wu, J.C., and Chung, C.C. (1985) *Appl. Catal.*, 16: 89.

[11] Chang, R.C. and Wang, I. (1987) *J. Catal.*, 107: 195.

[12] Hirashima, Y., Nishiwaki, K., Miyakoshi, A., Tsuiki, H., Ueno, A., and Nakabayashi, H. (1988) *Bull. Chem. Soc. Jpn*, 61: 1945.

[13] Fung, J. and Wang, I. (1991) *J. Catal.*, 130: 577.

[14] Mao, D., Lu, G., Chen, Q., Xie, Z., and Zhang, Y. (2001) *Catal. Lett.*, 77: 119.

[15] Mao, D., Chen, Q., and Lu, G. (2003) *Appl. Catal. A: Gen.*, 244: 273.

[16] Reddy, B.M., Reddy, E.P., Manohar, B., and Mehdi, S. (1992) *Advances in Catalyst Design*; World Scientific: Singapore, 196.

[17] Reddy, B.M., Reddy, E.P., and Manohar, B. (1993) *Langmuir*, 9: 1781.

[18] Lakshmi, J.L., Ihasz, N.J., and Miller, J.M. (2001) *J. Mol. Catal. A: Chem.*, 165: 199.

[19] Vishwanathan, V., Roh, H.-S., Kim, J.-W., and Jun, K.-W. (2004) *Catal. Lett.*, 96: 23.

[20] Manríquez, M.E., López, T., Gómez, R., and Navarrete, J. (2004) *J. Mol. Catal. A: Chem.*, 220: 229.

[21] Reddy, B.M., Reddy, E.P., and Manohar, B. (1993) *Appl. Catal. A: Gen.*, 96: L1.

[22] Reddy, B.M., Ganesh, I., and Reddy, E.P. (1997) *Res. Chem. Intermed.*, 23: 703.

[23] Reddy, B.M., Ganesh, I., Reddy, E.P., and Kumar, M.V. (1997) *Indian J. Chem. Technol.*, 4: 256.

[24] De Farias, R.F., Arnold, U., Martinez, L., Schuchardt, U., Jannini, M.J.D.M., and Airoldi, C. (2003) *J. Phys. Chem. Solids*, 64: 2385.

[25] Uchisawa, J.O-., Wang, S., Nanba, T., Ohi, A., and Obuchi, A. (2003) *Appl. Catal. B: Envir.*, 44: 207.

[26] Lin, W., Lin, L., Zhu, Y.X., Xie, Y.C., Scheurell, K., and Kemnitz, E. (2005) *J. Mol. Catal. A: Chem.*, 226: 263.

[27] Lu, C.M., Lin, Y.M., and Wang, I. (2000) *Appl. Catal. A: Gen.*, 198: 223.

[28] Kijenski, J., Winiarek, P., Paryjczak, T., Lewicki, A., and Mikolajska, A. (2002) *Appl. Catal. A: Gen.*, 233: 171.

[29] US Patent 5,576,467, 1996.

[30] Szalaty-Bujakowska, A., Kujawa, J., Ziolek, M., and Fiedorow, R. (2003) *Polish J. Chem.*, 77: 789.

[31] Barrera, M.C., Viniegra, M., Escobar, J., Vrinat, M., de los Reyes, J.A., Murrieta, F., and Garcia, J. (2004) *Catal. Today*, 98: 131.

[32] Weissman, J.G., Ko, E.I., and Katyal, S. (1993) *Appl. Catal. A: Gen.*, 94: 45.

[33] Maity, S.K., Rana, M.S., Bej, S.K., Juarez, J.A-., Murlidhar, G., and Rao, T.S.R.P. (2001) *Catal. Lett.*, 72: 115.

[34] Miciukiewicz, J., Mang, T., and Knözinger, H. (1995) *Appl. Catal. A: Gen.*, 122: 151.

[35] Tanabe, K.; Hattori, S.; Tanaka, Y.; Cho, K. (1990) JP 02048540.

[36] Yoshida, O.; Mori, Y.; Fujii, Y.; Okada, H.; Oguri, M. (2004) JP 2004323398.

[37] Cheng, G.-B., Lu, C.-X., and Peng, X.-H. (2002) *Yingyong Huaxue*, 19: 181.

[38] Reddy, B.M., Sreekanth, P.M., and Khan, A. (2002) *Bull. Catal. Soc. India*, 1: 58.

[39] Reddy, B.M., Sreekanth, P.M., and Khan, A. (2004) *Synth. Commun.*, 34: 1839.

[40] Sohn, J.R., Cho, H.S., and Kim, H.W. (1999) *J. Ind. Eng. Chem. (Seoul)*, 5: 1.

[41] Sohn, J.R. and Lee, J.S. (2003) *Bull. Korean Chem. Soc.*, 24: 159.

[42] Das, D., Mishra, H.K., Dalai, A.K., and Parida, K.M. (2004) *Catal. Lett.*, 93: 185.

[43] Machida, M., Ikeda, S., Kurogi, D., and Kijima, T. (2001) *Appl. Catal. B: Envir.*, 35: 107.

[44] Haneda, M., Kintaichi, Y., Inaba, M., and Hamada, H. (1998) *Catal. Today*, 42: 127.

[45] Haneda, M., Kintaichi, Y., Inaba, M., and Hamada, H. (1997) *Bull. Chem. Soc. Jpn.*, 70: 499.

[46] Mariscal, R., Rojas, S., Gomez-Cortes, A., Diaz, D., Perez, R., and Fierro, J.L.G. (2002) *Catal. Today*, 75: 385.

[47] Haneda, M., Kintaichi, Y., Inaba, M., and Hamada, H. (1997) *Appl. Surf. Sci.*, 121/122: 391.

[48] Haneda, M., Kintaichi, Y., Inaba, M., and Hamada, H. (1997) *Bull. Chem. Soc. Jpn.*, 70: 2171.

[49] Machida, M., Ikeda, S., and Kijima, T. (2003) *Stud. Surf. Sci. Catal.*, 145: 243.

[50] Jiang, X., Ding, G., Lou, L., Chen, Y., and Zheng, X. (2004) *J. Mol. Catal. A: Chem.*, 218: 187.

[51] Machida, M., Watanabe, T., Ikeda, S., and Kijima, T. (2002) *Catal. Commun.*, 3: 233.

[52] Lai, S.K., Zhang, H., and Ng, C.S. (2004) *Catal. Lett.*, 92: 106.

[53] Tajima, M., Niwa, M., Fujii, Y., Koinuma, Y., Aizawa, R., Kushiyama, S., Kobayashi, S., Mizuno, K., and Ohuchi, H. (1997) *Appl. Catal. B: Envir.*, 12: 263.

[54] Tajima, M., Niwa, M., Fujii, Y., Koinuma, Y., Aizawa, R., Kushiyama, S., Kobayashi, S., Mizuno, K., and Ohuchi, H. (1997) *Appl. Catal. B: Envir.*, 14: 97.

[55] Lai, S.K., Pan, W., and Ng, C.F. (2000) *Appl. Catal. B: Envir.*, 24: 207.

[56] Kataoka, S., Tompkins, D.T., Zeltner, W.A., and Anderson, M.A. (2002) *J. Photochem. Photobio. A: Chem.*, 148: 323.

[57] Zorn, M.E., Tompkins, D.T., Zeltner, W.A., and Anderson, M.A. (1999) *Appl. Catal. B: Envir.*, 23: 1.

[58] Yu, J.C., Lin, J., and Kwok, R.W.M. (1998) *J. Phys. Chem. B*, 102: 5094.

[59] Liu, S.W., Song, C.F., Lu, M.K., Wang, S.F., Sun, D.L., Qi, Y.X., Xu, D., and Yuan, D.R. (2003) *Catal. Commun.*, 4: 343.

[60] Navio, J.A., Colon, G., and Herrmann, J.M. (1997) *J. Photochem. Photobio. A: Chem.*, 108: 179.

[61] Navio, J.A., Gomez, M.G., Adrian, M.A.P., and Mota, J.F. (1993) In *Heterogeneous Catalysis and Fine Chemicals III*; Guisenet, M. et al., eds.; Elsevier, 431.

[62] Colon, G., Hidalgo, M.C., and Navio, J.A. (2002) *Appl. Catal. A: Chem.*, 231: 185.

[63] Navio, J.A., Hidalgo, M.C., Roncel, M., and De la Rosa, M.A. (1999) *Mat. Lett.*, 39: 370.

[64] Schattka, J.H., Shchukin, D.G., Jia, J., Antonietti, M., and Caruso, R.A. (2002) *Chem. Mater.*, 14: 5103.

[65] Zorn, M.E., Tompkins, D.T., Zeltner, W.A., and Anderson, M.A. (2000) *Environ. Sci. Technol.*, 34: 5206.

[66] Rengakuji, S., Nakamura, Y., and Hara, Y. (2001) *Electrochemistry*, 69: 764.

[67] Tauster, S.J., Funk, S.C., and Garten, R.L. (1978) *J. Am. Chem. Soc.*, 100: 170.

[68] Tauster, S.J., Funk, S.C., Baker, R.T.K., and Horsley, J.A. (1981) *Science*, 211: 1121.

[69] Moles, P.J. ed.; (1994) *Catal. Today (Special Issue)*; 20: 185 (and references therein).

[70] Reddy, B.M., Ganesh, I., and Choudhury, B. (1999) *Catal. Today*, 49: 115.

[71] Navio, J.A., Marchena, F.J., Macias, M., and Soto, P.J.S. (1992) *J. Mater. Sci.*, 27: 2463.

[72] Andrianainarivelo, M., Corriu, R.J.P., Leclercq, D., Mutin, P.H., and Vioux, A.J. (1997) *Mater. Chem.*, 7: 279.

[73] De Farias, R.F. and Airoldi, C.J. (1999) *Coll. Int. Sci.*, 220: 255.

[74] Khan, A., Ganesh, I., Madhavendra, S.S., and Reddy, B.M., unpublished results.

[75] Ferguson, J.D., Yoder, A.R., Weimer, A.W., and George, S.M. (2004) *Appl. Surf. Sci.*, 226: 393.

[76] Pajonk, G.M. (1991) *Appl. Catal.*, 72: 217.

[77] Bartlett, J.R., Gazeau, D., Zemb, Th., and Woolfrey, J.L. (1998) *Langmuir*, 14: 3538.

[78] Bartlett, J.R., Gazeau, D., Zemb, Th., and Woolfrey, J.L. (1997) *Prog. Colloid Polymer Sci.*, 105: 60.

[79] Manik, S.K., Dutta, H., and Pradhan, S.K. (2003) *Mater. Chem. Phys.*, 82: 848.

[80] Ganesh, I., Johnson, R., Mahajan, Y.R., Khan, A., Madhavendra, S.S., and Reddy, B.M. (2004) *J. Mater. Res.*, 19: 1015.

[81] Yang, P., Zhao, D., Margolese, D.I., Chmelka, B.F., and Stucky, G.D. (1998) *Nature*, 396: 152.

[82] Yuan, Z.-Y., Ren, T.-Z., Vantomme, A., and Su, B.-L. (2004) *Chem. Mater.*, 16: 5096.

[83] Reddy, B.M., Chowdhury, B., and Smirniotis, P.G. (2001) *Appl. Catal. A: Gen.*, 211: 19.

[84] Reddy, B.M., Chowdhury, B., Reddy, E.P., and Fernández, A.J. (2000) *Mol. Catal. A: Chem.*, 162: 431.

[85] Reddy, E.P., Rojas, T.C., Fernandez, A., Choudhury, B., and Reddy, B.M. (2000) *Langmuir*, 16: 4217.

[86] Reddy, B.M. and Choudhury, B. (1998) *J. Catal.*, 179: 413.

[87] Reddy, B.M., Choudhury, B., Ganesh, I., Reddy, E.P., Rojas, T.C., and Fernández, A.J. (1998) *Phys. Chem. B*, 102: 10176.

[88] Reddy, B.M., Manohar, B., and Mehdi, S.J. (1992) *Solid State Chem.*, 97: 233.

[89] Reddy, B.M., Reddy, E.P., Srinivas, S.T., Mastikhin, V.M., Nosov, A.V., and Lapina, O.B. (1992) *J. Phys. Chem.*, 96: 7076.

[90] Park, E.U., Lee, M.H., and Sohn, J.R. (2000) *Bull. Korean Chem. Soc.*, 21: 913.

[91] Lopez, J.G., Pastenes, H.P., Gaytan, J.T., and Garcia, T.V. (2002) *Revista Mexicana de Ingenieria Quimica*, 1: 29.

[92] Mao, D., Lu, G., and Chen, Q. (2004) *Appl. Catal. A: Gen.*, 263: 83.

[93] Sohn, J.R. and Lee, S.H. (2004) *Appl. Catal. A: Gen.*, 266: 89.

[94] Zou, H. and Lin, Y.S. (2004) *Appl. Catal. A: Gen.*, 265: 35.

[95] Machida, M. and Ikeda, S. (2004) *J. Catal.*, 227: 53.

[96] Lonyi, F. and Valyon, J. (1996) *J. Thermal Anal.*, 46: 211.

[97] Noguchi, T. and Mizuno, M. (1967) *Sol. Energy*, 11: 56.

[98] Brown Jr, F.H. and Pol Duwez, J. (1954) *Amer. Ceram. Soc.*, 37: 129.

[99] Coughanour, L.W., Roth, R.S., and De Prosse, V.A. (1954) *J. Res. Nat. Bur. Stand.*, 52: 37.

[100] Cocco, A. and Torriano, G. (1965) *Ann. Chim (Rome)*, 55: 153.

[101] Newnham, R.E. (1967) *J. Amer. Ceram. Soc.*, 50: 216.

[102] Park, Y. (1998) *Mat. Res. Bull.*, 33: 1325.

[103] Shibata, K., Kiyoura, T., Kitagawa, J., Sumiyoshi, T., and Tanabe, K. (1973) *Bull. Chem. Soc. Jpn.*, 46: 2985.

[104] Tanabe, K., Sumiyoshi, T., Shibata, K., Kiyoura, T., and Kitagawa, J. (1974) *Bull. Chem. Soc. Jpn.*, 47: 1064.

[105] Tanabe, K. (1970) *Solid Acids and Bases: Their Catalytic Applications*; Academic Press: New York.

[106] Tanabe, K. (1981) *Catalysis Science and Technology*; Anderson, J.R. and Boudart, M., eds.; Springer-Verlag: New York; Vol. 2, 231.

[107] Kung, H.H. (1984) *J. Solid State Chem.*, 52: 191.

[108] Fung, J. and Wang, I. (1996) *J. Catal.*, 164: 166.

[109] Fung, J. and Wang, I. (1998) *Appl. Catal. A: Gen.*, 166: 327.

[110] Walvekar, S.P., Halgeri, A.B., Ramanna, S., and Srinivasan, T.N. (1976) *Fertilizer Technol.*, 13: 241.

[111] Solinas, V. and Ferno, I. (1998) *Catal Today*, 41: 179.

[112] Bond, G.C. (1987) *Heterogeneous Catalysis: Principles and Applications*; Oxford University Press: Oxford.

[113] Santos, J., Phillips, J., and Dumesic, J.A. (1983) *J. Catal.*, 81: 147.

[114] Sun, Y.M., Belton, D.N., and White, J.M. (1986) *J. Phys. Chem.*, 90: 5178.

[115] Bond, G.C., Sarkany, A.I., and Parfitt, G.D. (1979) *J. Catal.*, 57: 476.

[116] Bond, G.C. and Tahir, S.F. (1991) *Appl. Catal.*, 71: 1.

[117] Lin, J. and Yu, J.C. (1998) *J. Photochem. Photobiol. A: Chem.*, 116: 63.

[118] Anderson, C. and Bard, A.J. (1994) *J. Phys. Chem.*, 98: 1769.

[119] Reddy, B.M., Sreekanth, P.M., Yamada, Y., Xu, Q., and Kobayashi, T. (2002) *Appl. Catal. A: Gen.*, 228: 269.

[120] Massoth, F.E. (1978) *Adv. Catal.*, 27: 265.

[121] Knözinger, H. (1988) Proc. 9th Intern. Congr. Catal., Calgary, 1988. In Philips, M.J. and Ternan, M., eds.; Chem. Inst.: Ottawa, Canada; Vol. 5, 20.

[122] Lee, E.H. (1963) (to Monsanto Chemical) French Patent 1,323,317, April 5.

[123] Feil, F.S., Van Ommen, J.S., and Ross, J.R.H. (1987) *Langmuir*, 3: 668.

[124] Chung, J.S., Miranada, R., and Bennett, C.O. (1988) *J. Catal.*, 114: 398.

[125] Yang, T.J. and Lunsford, J.H. (1987) *J. Catal.*, 103: 55.

[126] Burcham, L.J., Deo, G., Gao, X., and Wachs, I.E. (2000) *Top. Catal.*, 11/12: 85.

[127] Hawker, P., Myers, N., Huthwohl, G., Vogel, H.T., Bates, B., Magnusson, L., and Bronnenberg, P. (1997) SAE Technical Paper Series, 970182.

[128] Farrauto, R., Voss, K.E., and Heck, R.M. (1993) SAE Technical Paper Series, 932720.

[129] Cooper, B.J. and Thoss, J.E. (1989) SAE Technical Paper Series, 890404.

[130] Chou, P. and Vannice, M.A. (1987) *J. Catal.*, 107: 129.

[131] Boudart, M., Aldog, A.W., and Vannice, M.A. (1970) *J. Catal.*, 18: 46.

[132] Lin, S.D. and Vannice, M.A. (1993) *J. Catal.*, 143: 539.

[133] Greene, T.W. and Wuts, P.G.M. (1991) *Protective Groups in Organic Synthesis*, 2nd ed.; Wiley and Sons, Inc.: New York, 175.

[134] Reddy, B.M. and Sreekanth, P.M. (2003) *Tetrahedron Lett.*, 44: 4447.

[135] Reddy, B.M. and Sreekanth, P.M. (2002) *Synth. Commun.*, 32: 2815.

[136] Reddy, B.M., Reddy, V.R., and Giridhar, D. (2001) *Synth. Commun.*, 31: 1819.

[137] Arata, K. (1990) *Adv. Catal.*, 37: 165 and references therein.

[138] Wang, W.-J., Qiao, M.-H., Li, H.-X., Dai, W.-L., and Deng, J.-F. (1998) *Appl. Catal. A: Gen.*, 169: 151.

[139] Scheithauer, M., Grasselli, R.K., and Knözinger, H. (1998) *Langmuir*, 14: 3019.

[140] Hadjiivanov, K.I. and Klissurski, D.G. (1996) *Chem. Soc. Rev.*, 25: 61 and references therein.

[141] Anpo, M. (2004) *Bull. Chem. Soc. Jpn.*, 77: 1427 and references therein.

[142] Reddy, E.P., Sun, B., and Smirniotis, P.G. (2004) *J. Phys. Chem. B*, 108: 17198.